

---

## ELICITATION SUMMARY

**BRENDA J. LITTLE**

*Note: Because of Dr. Little's specialized expertise, her elicitation focused on the processes and potential impacts of microbiologically influenced corrosion (MIC) on waste package degradation.*

### OVERVIEW OF MIC PROCESSES

The potential for microbiologically influenced corrosion (MIC) is directly related to biofilm formation, which is controlled by the availability of nutrients, water, and electron acceptors. Absence of any one of these will preclude microbial growth and therefore MIC. During the early stages of the repository's use, elevated temperatures and low relative humidity will inhibit growth of microbes and their influence on corrosion. The expected temperatures are not high enough to sterilize the repository, so that microbes will survive but not grow during the early hot, dry period. As temperatures decline to below about 100°C and relative humidity increases above 60 percent, the potential for MIC begins.

The most systematic way to understand the potential for microbial growth, to establish the limiting conditions, and to assess the potential for MIC is through a mass balance inventory of the potential repository. Such mass balances were developed for Canadian (Stroes-Gascoyne, 1989) and Swiss (McKinley and Grogan, 1991) repositories. Biomass will be inherently limited by some essential nutrient (C, N, P, S, etc.). A mass balance that includes a complete material inventory, identifying naturally occurring nutrients as well as those introduced in buffer and backfill, and an evaluation of energy-producing reaction provides a conservative estimate of the maximum microbial growth that can be sustained in the repository. Much of the inventory will be refractory, so that all materials cannot be assimilated by microorganisms. Similarly, not all redox reactions that can be defined will be

used by the organisms. After the microbial population has been modeled, the potential for MIC can be assessed by evaluating container material, environmental conditions, and mechanisms that would lead to MIC. For example, a time-history for temperature and relative humidity, as well as the assessed potential for water drips on the waste packages, are important in assessing potential for MIC at Yucca Mountain.

Although several types of microbes have been isolated from Yucca Mountain and grown in laboratory conditions, they grow because they are provided with water, abundant nutrients, and electron acceptors. In the natural environment, there is a difference between survival and growth. Microorganisms can withstand long periods of starvation and desiccation. Without a mass balance for the repository, it is unknown whether organisms isolated and grown under laboratory conditions will, in fact, grow under repository conditions. Subsurface bacteria are stressed. Growth rates typically are 2- to 1000-fold lower than growth rates measured in surface soils. For now, we must compare expected environmental conditions in the repository with the cases of MIC that have been documented under various conditions, and then make a judgment about the likelihood that MIC will occur under changing conditions at the potential repository. After temperatures decline below about 100°C and relative humidity increases to more than 60 percent, the potential for microbial growth will be affected greatly by the possibility of drips on the waste package. Unless microbes can use nutrients in the surrounding rock matrix, their activities are limited by nutrients transported by groundwater and drips. If dripping is intermittent and leads to alternating wetting and drying periods, microbes may survive dry periods but will grow only during the wet periods. Drilling fluids, diesel fuels, hydraulic fluids, and gaseous exhausts can be degraded by microorganisms in the presence of water.

Below I consider several causative organisms, possible mechanisms for MIC, and their relationship to Yucca Mountain isolates, followed by my assessment of how MIC should be considered in modeling of waste package degradation.

---

## MECHANISMS FOR MIC

It is established that the most devastating microbiologically influenced corrosion (MIC) takes place in the presence of microbial consortia in which many physiological types of bacteria, including metal-oxidizing bacteria, sulfate-reducing bacteria (SRB), acid-producing bacteria, and metal-reducing bacteria (MRB), interact in complex ways within the structure of biofilms (Little et al., 1991) (Figure BL-1). MIC does not produce a unique form of localized corrosion. Instead, MIC can result in pitting, crevice corrosion, and underdeposit corrosion, in addition to enhanced galvanic and erosion corrosion. The principal effect of MIC under aerobic conditions is to increase the probability that localized corrosion will be initiated, rather than to affect the rate of corrosion once it has begun. That is, MIC can set up the proper conditions for pitting or crevice corrosion. Once localized corrosion has been initiated, MIC can maintain proper conditions (e.g., low oxygen, low pH) for continued pit/crevice growth. However, the rate at which pits/crevices propagate is not governed by the presence of microorganisms. Under anaerobic, reducing conditions, aggressive MIC is observed when there is some mechanism for the removal or transformation of corrosion products (i.e., there are switches from stagnation to flow or from anaerobic to aerobic conditions). Therefore, in the models of corrosion of the carbon steel outer barrier and the corrosion-resistant inner barrier, MIC should be considered in the evaluation of the probability of initiation and, equivalently, the pit/crevice density. Likewise, the spatial distribution of MIC should be considered in modeling the spatial distribution of corrosion, for example, in estimating how large biofilms can become and where the proper conditions exist for microbial growth (e.g., dripping water conditions). If concentrations of salts develop on the surface of the waste package in response to dripping followed by evaporation, those areas may not be conducive to microbial growth even when wet. I am not sure what the effect of 1000x J-13 water would have on the potential for growth.

---

## METAL-OXIDIZING BACTERIA

### Manganese Oxidation

Manganese oxidation is coupled to cell growth and metabolism of organic carbon. Although the reduced form of manganese, generally identified as  $Mn^{2+}$ , is soluble, the various oxidized forms,  $Mn_2O_3$ ,  $MnOOH$ ,  $Mn_3O_4$ ,  $MnO_2$ , are insoluble. As a result of microbial action, manganese oxide deposits are formed on submerged materials, including metal, stone, glass, and plastic, and can occur in natural waters that have manganese concentrations as low as 10 to 20 ppb.

Deposition rates of  $1 \text{ mcoul cm}^{-2} \text{ day}^{-1}$  have been observed (Dickinson and Lewandowski, 1996). Microbially deposited manganese oxide on stainless steel in fresh water caused an increase in  $E_{\text{corr}}$  and increased cathodic current density at potentials above -200 mV (vs saturated calomel reference electrode [SCE]). For mild steel corrosion under anodic control, the oxides can elevate corrosion current, but will cause little positive shift in  $E_{\text{corr}}$ . The increase in corrosion current may be significant, particularly for mild steel covered with biomineralized oxides and corrosion products that provide large mineral surface areas. Given sufficient conductivity in the deposits, much of the material may serve as an oxide cathode to support corrosion at the oxygen-depleted anode. Continued biomineralization may sustain a significant amount of the cathodic current. Both factors can increase the risk of stainless steel corrosion. Ennobled  $E_{\text{corr}}$  can exceed pitting potentials for low-molybdenum alloys, enhancing risk of pit nucleation, while elevated cathodic current density impedes repassivation. Biomineralized manganic oxides are efficient cathodes that increase cathodic current density on stainless steel by several decades at potentials between roughly -200 and +400 mV<sub>SCE</sub>. The extent to which the elevated current density can be maintained is controlled by the electrical capacity of the mineral, reflecting both total accumulation and conductivity of the mineral-biopolymer assemblage (only material in electrical contact with the metal will be cathodically active). Oxide accumulation is controlled by the biomineralization rate and the corrosion current, in that high corrosion currents will discharge

the oxide as rapidly as it is formed. Manganese oxidizers were not evaluated in the microbiology of the potential Yucca Mountain repository (Section 2.6, Horn and Jones).

### **Iron Oxidation**

Iron-oxidizing bacteria produce orange-red tubercles of iron oxides and hydroxides by oxidizing ferrous ions from the bulk medium or the substratum. Iron-depositing bacteria are microaerophilic and may require synergistic associations with other bacteria to maintain low oxygen conditions in their immediate environment. Deposits of cells and metal ions create oxygen-concentration cells that effectively exclude oxygen from the area immediately under the deposit and initiate a series of events that individually or collectively are very corrosive. In an oxygenated environment, the area immediately under individual deposits becomes deprived of oxygen. That area becomes a relatively small anode compared to the large, surrounding oxygenated cathode. Cathodic reduction of oxygen may result in an increase in pH of the solution in the vicinity of the metal. The metal will form metal cations at anodic sites. If the metal hydroxide is the thermodynamically stable phase in the solution, the metal ions will be hydrolyzed by water, forming  $H^+$  ions. If cathodic and anodic sites are separated from one another, the pH at the anode will decrease and that at the cathode will increase. The pH at the anode depends on specific hydrolysis reactions. In addition,  $Cl^-$  ions from the electrolyte will migrate to the anode to neutralize any buildup of charge, forming heavy metal chlorides that are extremely corrosive. Under these circumstances, pitting involves the conventional features of differential aeration, a large cathode-to-anode surface area, and the development of acidity and metallic chlorides. Pit initiation depends on mineral deposition by bacteria. Pit propagation is dependent not on activities of the organisms, but on metallurgy. Iron-oxidizing bacteria were cultured from Yucca Mountain tuff (Section 2.6, Horn and Jones). Tubercle formation was not reported.

### **SULFATE-REDUCING BACTERIA**

Sulfate-reducing bacteria (SRB) are a diverse group of anaerobic bacteria that can be isolated from a variety of environments, especially seawater in which the concentration of sulfate is

typically 25 mM (Postgate, 1979). Even though the oxygen content of seawater above the thermocline ranges from 5 to 8 ppm, anaerobic microorganisms survive in anaerobic microniches until conditions are suitable for their growth. During biofilm formation, if the aerobic respiration rate within a biofilm is greater than the oxygen diffusion rate, the metal/biofilm interface can become anaerobic and provide a niche for sulfide production by SRB (Figure BL-2). The critical thickness of the biofilm required to produce anaerobic conditions depends on the availability of oxygen and the rate of respiration.

The corrosion rate of iron in the presence of hydrogen sulfide is accelerated by the formation of iron sulfide minerals that stimulate the cathodic reaction through a decrease in hydrogen overvoltage at cathodic sites. Once electrical contact is established, mild steel behaves as an anode, and electron transfer occurs through the iron sulfide. In the absence of oxygen, the metabolic activity of SRB causes accumulation of hydrogen sulfide near metal surfaces. This is particularly evident when metal surfaces are covered with biofilms. The concentration of sulfide is highest near the metal surface, where iron sulfide forms quickly and covers the steel surface if both ferrous and sulfide ions are available. At low ferrous ion concentrations, adherent and temporarily protective films of iron sulfides are formed on the steel surface, with a consequent reduction in corrosion rate. High rates of SRB-induced corrosion of mild steel are maintained only in high concentrations of ferrous ion. Observations have shown that in anaerobic conditions, SRB can enhance corrosion by factors of three to five.

However, aggressive SRB corrosion requires a source of soluble ferrous ions and exposure to oxygen. For example, Hardy and Bown (1984) demonstrated that corrosion rates of mild steel in anaerobic cultures of SRB were low ( $1.45 \text{ mg/dm}^2/\text{day}$ ). Subsequent exposure to air caused high corrosion rates ( $129 \text{ mg/dm}^2/\text{day}$ ).

The impact of sulfides on the corrosion of copper alloys has received considerable attention, including published reports documenting localized corrosion of copper alloys by SRB in estuarine environments (Little et al., 1988, 1989) and a report of the failure of copper alloys in polluted seawater containing waterborne sulfides that stimulate pitting and stress corrosion cracking (Rowlands, 1965). Copper alloys suffer accelerated corrosion attack in seawater containing 0.01 ppm sulfide after a one-day exposure (Gudas and Hack, 1979). Copper ions

---

migrate through the layer, react with more sulfide, and produce a thick, black scale. High corrosion rates of copper alloys in the presence of SRB require flow to remove sulfide layer and expose more base metal to oxide/sulfide formation or the introduction of oxygen.

SRB were not isolated from the Exploratory Studies Facility (ESF) at Yucca Mountain. The sulfate concentration in J-13 water is 0.17 to 0.32 mM. SRB concentrations are always correlated with groundwater sulfate concentration. The distribution of favorable pH conditions ranges from 6 to 12, although they have been known to mutate to accommodate pH conditions. The limiting factor regarding SRB activity in the potential repository probably will be the prevalence of oxygen (especially after the repository has cooled down) and the lack of sulfate and water except, perhaps, under dripping conditions. Yucca Mountain bacterial isolates were capable of sulfide production through a process of putrefaction when provided with excess protein, an unlikely situation at the potential repository.

### **METAL-REDUCING BACTERIA**

Dissimilatory iron and/or manganese reduction occurs in several microorganisms, including anaerobic and facultative aerobic bacteria. Inhibitor and competition experiments suggest that Mn(IV) and Fe(III) are efficient electron acceptors that are similar to nitrate in redox ability and are capable of out-competing electron acceptors of lower potential, such as sulfate or carbon dioxide (Myers and Nealson, 1988). Many of the recently described MRBs are capable of using a variety of electron acceptors, including nitrate and oxygen. Iron and manganese-reducing microorganisms must be in direct contact with oxides to reduce them.

Obuekwe et al. (1981) evaluated corrosion of mild steel under conditions of simultaneous formation of ferrous and sulfide ions. They reported extensive pitting when both processes were active. When only sulfide was produced, corrosion rates increased initially but later declined due to formation of a protective FeS film. High amounts of soluble iron prevent formation of protective sulfide layers on ferrous metals. Iron recycling commonly is

observed within a sediment system: iron is oxidized at the surface from  $Fe^{+2}$  to  $Fe^{+3}$  under aerobic conditions. Solid phases containing  $Fe^{+3}$  (hematite, goethite, etc.) precipitate due to their lower solubilities. With increasing depth in the sediments, microbes make the conditions progressively less aerobic, and iron is reduced back to  $Fe^{+2}$ . With flow and removal, the dissolved ferrous iron species are transported to the surface, once again oxidized, and the cycle begins again. As many as 300 cycles can occur in lake and sea water sediments. The process, which requires flow and removal of material, may occur within a pit that is subject to persistent dripping conditions. Iron-reducing bacteria operate within the pit to reduce the iron, which then is removed and replaced by oxidized iron. Suppression of pH is not an important consideration in this process. Because of the expected aerobic conditions and the potential for dripping, iron-reduction could be extremely important under conditions at Yucca Mountain. Iron-reducing bacteria were isolated from the ESF, but have not been used in corrosion experiments.

In considering the potential impact that a thick iron oxide layer might have on microbial growth, or a thick section of corrosion products left as the CAM corrodes, I conclude that microbes can permeate the corrosion products. One can expect to find microorganisms wherever one finds water. The ease with which the corrosion products are permeated will depend on the surface area and the crystal structure of the iron oxide (e.g., hematite vs. goethite). Fe-reducing bacteria can grow efficiently in the presence of less crystalline corrosion products that could retain more water. If the corrosion products have a high ability to hold water (due to drips and surface characteristics), the potential for MIC will be enhanced.

#### **ACID-PRODUCING AND SLIME-PRODUCING BACTERIA**

Acid production and slime production will not be discussed at any length. Both were evaluated by Horn and Jones (1997) for isolates from the Yucca Mountain ESF. Both processes required the addition of glucose to the growth medium, a highly unlikely circumstance at the potential repository. The lowest pH attained under altered conditions was

---

4.46, a number that could be used for any modeling that requires an extreme pH value. Slime production is important in that it provides the matrix for biofilm formation. In summary, acid and slime production will be a consideration only with the inclusion of an assimilable carbon source identified while developing assumptions and conclusions regarding mass balance.

## FUNGI

Fungi are aerobic, can grow in a humid atmospheric environment, can survive desiccation/starvation, and flourish when conditions are favorable. Vault conditions seem ideally suited for the proliferation of fungi. The water activity ( $a_w$ ) for Yucca Mountain is 0.65. Bacteria require  $a_w$  in the range 0.90 to 0.95. Fungi thrive at  $a_w = 0.65$ . In addition, some fungi are thermophilic or thermotolerant, growing at temperatures of 50°C or above. Desert soils and rocks provide habitats for thermophilic fungi. Fungi produce acids (pH reduction to 4.6 has been observed in experiments) and have caused serious corrosion problems in aluminum and carbon steel. Fungi were not isolated by Penny et al. in the microbial inventory of the ESF. Fungi commonly are found growing on materials high in organics (e.g., composts, stored grain, wax, and hydrocarbons) and at the water/fuel interface in petroleum transportation and storage systems. The potential for fungal growth illustrates the need for a mass balance inventory for the potential repository. There may be insufficient organic carbon, nitrogen, and/or phosphorous to sustain fungi growth.

## ENNOBLEMENT

Ennoblement is the positive shift in corrosion potential of a metal, such as stainless steel or a nickel alloy, as it becomes more noble with exposure time. Ennoblement in fresh water systems has been associated with a specific group of microorganisms, manganese-depositing bacteria. In summary, manganese oxide biodeposition on stainless steel surfaces forces a shift in the positive, more noble direction, moving the corrosion potential above the pitting potential and making some stainless steels more vulnerable to pitting and crevice corrosion.

It is well documented that the corrosion of stainless steels is more severe in natural seawater than in sterile chloride-containing media, and investigators agree that the increased corrosion is due to ennoblement in the presence of a biofilm. However, no specific organisms have been identified. The mechanism for ennoblement in seawater systems requires a more detailed discussion. Typically,  $E_{\text{corr}}$  of a stainless steel coupon exposed to natural seawater begins to increase 15 to 30 mV/day within 1 to 5 days after immersion. Steady-state potentials of 200 to 400 mV (SCE) are attained after exposure periods ranging from about 10 days to 8 to 10 weeks.  $E_{\text{pit}}$  for type 304 stainless steel in abiotic solutions at seawater chloride levels of 0.5 M is -50 mV (SCE), slightly higher than typical initial  $E_{\text{corr}}$  values for stainless steel in natural seawater. This suggests that even slight ennoblement can increase the risk of localized corrosion, which occurs when  $E_{\text{corr}}$  reaches the value of  $E_{\text{pit}}$ . In practice, localized corrosion of type 304 stainless steel in seawater has been observed at potentials of about +250 mV (SCE). Numerous researchers have shown that increased cathodic reaction rates accompany ennoblement of  $E_{\text{corr}}$ . The nature of the processes leading to accelerated cathodic reaction rates is not known. For neutral, aerated solutions, the cathodic reaction is reduction of oxygen.

Early attempts to explain increased cathodic reaction rates used thermodynamic arguments that either a decrease in pH at the metal/biofilm interface or an increase of the partial pressure of oxygen ( $p_{\text{O}_2}$ ) raises the reversible potential,  $E_{\text{O}}^0$ , of the oxygen electrode. For aerobic biofilms, changes in  $E_{\text{O}_2}^0$  due to changes in  $p_{\text{O}_2}$  would be small. For seawater, a decrease of local pH from 8 to 3 would account for an ennoblement of about 300 mV, assuming that the exchanges of the current density ( $i_{\text{O}_2}^0$ ) for the oxygen-reduction reaction and the cathodic Tafel slope remain constant. When Little et al. (date?) measured  $E_{\text{pit}}$  in abiotic chloride solutions at pH = 4 and 2, they observed that  $E_{\text{pit}}$  decreased below ennobled  $E_{\text{corr}}$  values in natural seawater and therefore dismissed the possibility that ennoblement is due to reduction of surface pH.

---

The rate of oxygen reduction at a given potential ( $E$ ) can also increase in response to an increase of  $i_{O_2}^0$  that leads to an increase of  $E_{corr}^1$  to  $E_{corr}^3$ . Dexter and Gao (1988) suggested that increased oxygen-reduction rates may be due to an increase of  $i_{O_2}^0$ , mediated by biopolymer metal complexes known to catalyze oxygen reduction. The nature of these organometallic catalysts has been widely discussed. The mechanism of organometallic catalysis has been criticized, however, because ennoblement is observed on more noble metals, including titanium and platinum, which lack the transition elements thought to be necessary to form catalyzing complexes.

Molybdenum content may influence ennoblement. Furthermore, ennoblement occurs at a slower rate and to a lesser extent on titanium than on stainless steels. It is also possible that microorganisms change the rate-determining step in an electrochemical reaction or produce an entirely different mechanism. Chandrasekaran and Dexter (1993) suggested that reduction in surface pH and production of hydrogen peroxide at low oxygen concentrations are important contributory factors for ennoblement. Peroxide concentrations in the necessary ranges for ennoblement have not been measured for natural biofilms. Another possible cathodic reaction is the direct reduction of  $H_2S$ . Reduction of  $H_2S$  on iron produces  $FeS$ , which acts as a cathode having lower oxygen overvoltage than Fe.

## **EFFECT OF MIC ON PROBABILITY OF INITIATION AND RATE OF CORROSION**

### **Probability of MIC on Carbon Steel**

The microbial processes described above require temperatures below  $100^\circ C$ . Thermophiles readily grow at  $60^\circ C$  and can adapt to temperatures as high as the boiling point of water. Therefore, it is likely that microorganisms will adjust to  $60^\circ$  to  $80^\circ C$  in the potential repository. In addition, dripping water may provide nutrients and additional organisms.

My assessment of the probability of microbial growth of the existing repository population as a function of temperature for dripping and non-dripping conditions is given in Figure BL-3. The assumptions are that (1) some microorganisms have survived temperatures in excess of 100°C; (2) drips provide water and nutrients, not additional organisms; and (3) the repository is cooling. As the repository cools to 100°C, the probability of microbial growth becomes finite, but low. Based on our experience, there will be few survivors from the natural population (before emplacement of nuclear wastes). With further cooling to 60°C, the probability of growth under dripping conditions becomes relatively high (0.8). Given the long periods involved, I would expect adaptation to enable growth in what would otherwise be inhospitable temperatures. The progressive decline in probability with decreasing temperature reflects my expectation that, as discussed above, microbes adapted to elevated temperatures (thermophiles) have lower growth probability with decreasing temperature. Joanne Jones-Meehan (NRL, personal communication) recently completed studies with thermophilic bacteria from Yellowstone National Park. Those isolates, adapted over millennia to high temperatures, grew best at 100° to 102°C. As culture temperatures decreased, growth started to decrease around 80°C, growth decreased abruptly at 60°C, and cells died at 45°C. If additional organisms are being transported with the dripping water and nutrients, their growth potential should be addressed by mass balance considerations. It should be noted that the probability of microbial growth is greater than the probability of MIC. To arrive at the probability for MIC, one must look at the mass balance and the mechanisms that might lead to MIC.

#### **Effect of MIC on Carbon Steel**

Iron-reducing bacteria may be the most important organisms to consider in terms of MIC of carbon steel because (1) they were isolated from the ESF; (2) they could survive a humid environment if isolated within dense, wet corrosion layers; and (3) with adequate nutrients and anaerobic conditions, they could reduce ferric iron to ferrous. However, before their impact can be considered seriously, a mechanism must be described for the removal of reduced ferrous iron. Otherwise the ferrous ions would be reoxidized immediately in the aerobic environment of the potential repository. One could envision mini-pits that provide

iron recycling within very small areas. In laboratory experiments in the presence of *Shewanella putrefaciens*, the corrosion rate of carbon steel was 3 to 5 times greater than for abiotic controls.

#### **Effect of MIC on Corrosion-Resistant Materials**

The assessment of the potential for MIC to affect the candidate corrosion-resistant materials (alloy 625 and C-22) is quite uncertain, because there are no documented cases involving these alloys. For alloy 825, there is a single documented case of underdeposit corrosion (Brennenstuhl et al, 1990). It is likely that pitting susceptibility was enhanced by ennoblement. It generally is concluded that if a biofilm is present there is a higher likelihood of underdeposit corrosion.

Figure BL-4 presents my assessment of the probability of localized corrosion of the CRM due to MIC, assuming optimum temperatures of 60°C and dripping conditions. The probability of growth (0.8) was discussed previously. Given that growth occurs, the probability that a biofilm will develop on the CRM is relatively low (0.2), because of the difficulty of developing a significantly large biofilm beneath the thick layer of corrosion products (as much as 10 cm<sup>3</sup>) from the corroded CAM. Given that a biofilm develops, the potential for ennoblement is judged to be relatively high (0.5), since most materials become ennobled in the presence of a biofilm.

Given that ennoblement occurs, the probability of localized corrosion differs between alloys 625 and C-22. I estimate a probability of 0.6 that 625 would undergo localized corrosion given ennoblement, because the pitting potential for this alloy is within the range of the maximum open-circuit potential (300 to 350mV) that ennoblement may develop. Because the pitting potential of C-22 is higher, I estimate a low probability (0.1) of localized corrosion of this alloy. Given that localized corrosion does initiate, the rates (pit/crevice growth rates) should then be used for each alloy in modeling the degradation process. In the non-dripping case, the probability of localized corrosion of these corrosion-resistant alloys due to MIC is judged to be zero because of the lack of sufficient nutrients.

**Monel 400**

Monel 400 is being considered as an alternative corrosion-allowance material. Experience in stagnant seawater and polluted water showed that Monel 400 is susceptible to SRB-influenced corrosion, and de-alloying of the nickel has been reported in fluctuating no flow/flow conditions or alternating anaerobic/aerobic conditions. Standing stagnant water is unlikely in the repository in the absence of flooding. Small pools of stagnant water are possible. Iron-reducing bacteria will not be a problem for copper alloys. As with carbon steel, a thick biofilm is required (particularly in aerobic conditions) for SRB activity to lead to localized corrosion. My assessment of the probability of localized corrosion for carbon steel and Monel 400 due to SRB is given in Figure BL-5.

My assessment of the probability of developing a biofilm on either the carbon steel or Monel 400 outer barrier, given dripping conditions and temperatures of 60°C, is about 0.5, somewhat lower than predicted for non-copper-containing materials. Given that a biofilm develops, the probability that sulfide production by SRB will occur is judged to be low (0.1). This is because of the oxygenated conditions, the need for a thick biofilm to allow for anaerobic conditions, and the expected small amount of sulfate that would be available. Given that sulfides are produced by SRB, the potential for localized corrosion differs somewhat between Monel 400 and carbon steel. In the case of Monel 400, the probability of the initiation of localized corrosion due to the presence of sulfides is judged to be 0.6; for carbon steel it is 0.7. The probability of initiation for carbon steel is somewhat higher because it should be easier to achieve anaerobic conditions within the corrosion products that form on the carbon steel. Given that localized corrosion does initiate, the growth rate will proceed at the abiotic rate for each metal. Sanders and Maxwell (1983) found that, when exposed to seawater, Monel 400 was fouled by SRB at the same rate as Corten A steel. However, it took much longer to achieve a stable sulfate-reduction rate on Monel than on steel. Corrosion rates were similar, and the surfaces were characterized by deep pitting.

## **OTHER ISSUES**

### **Welds**

Microbes attach preferentially to roughed areas, including welds. Welds on 304 and 316 stainless steels show selective attack by iron-oxidizing bacteria. I do not expect bacteria to increase the probability for localized corrosion of the materials under discussion.

## **RECOMMENDED TESTS**

An attempt should be made to determine the effect of a concentrated salt solution (1000X J-13) on the growth of ESF isolates. Experiments should replicate the expected condition of drips on salt deposits left from evaporation on the waste packages. Microbial growth in 1000C = J13 should also be evaluated at 100°C.

## **REFERENCES**

- Brennenstuhl, A.M., Doherty, P.E., King, P.J., and Dunstall, T.G., 1990, The effects of biofouling on the corrosion of nickel heat exchanger alloys at Ontario Hydro, *in* Dowling, N.J., Mittleman, M.W., and Danko, J.C. (eds.), *Microbiologically Influenced Corrosion and Biodeterioration: The University of Tennessee, Knoxville*, p. 4-25 to 4-31.
- Chandrasekaran, P., and Dexter, S.C., 1993, Paper no. 493, *Corrosion/93, NACE*.
- Dexter, S.C., and Gao, G.Y., 1988, *Corrosion*, v. 44, p. 717.
- Dickinson, W.H., and Lewandowski, Z., 1996, Manganese biofouling and the corrosion behavior of stainless steel: *Biofouling*, v. 10, p. 79-93.
- Gudas, J.P., and Hack, H.P., 1979, Sulfide-induced corrosion of copper-nickel alloys: *Corrosion*, v. 35, p. 67-73.
- Hardy, J.A., and Bown, J.L., 1984, The corrosion of mild steel by biogenic sulfide films exposed to air: *Corrosion*, v. 40, p. 650.

- Little, B., Wagner, P., and Jacobus, J., 1988, The impact of sulfate-reducing bacteria on welded copper-nickel seawater piping systems: *Mat Perf*, v. 27, no. 8, p. 57-61.
- Little, B., Wagner, P., Jacobus, J., and Janus, L., 1989, Evaluation of microbiologically induced corrosion in an estuary: *Estuaries*, v. 12, no. 3, p. 138-141.
- McKinley, I.G., and Grogan, H.A., 1991, Consideration of microbiology in modelling the near field of a L/ILW repository: *Experientia*, v. 47, p. 573.
- Myers, C., and Neelson, K.H., 1988, Bacterial manganese reduction and growth with manganese oxide as the sole electron acceptor: *Science*, v. 240, p. 1319-1321.
- Obuekwe, C.O., Westlake, D.W.S., Plambeck, J.A., and Cook, F.D., 1981: Corrosion of mild steel in cultures of ferric iron reducing bacterium isolated from crude oil—I, polarization characteristics: *Corrosion*, v. 37 no. 8, p. 461-467.
- Postgate, J.R., 1979, *The Sulphate-Reducing Bacteria*: Cambridge University Press, Cambridge, UK.
- Rowlands, J.C., 1965, Corrosion of tube and pipe alloys due to polluted seawater: *Journal of Applied Chemistry*, v. 15, p. 57-63.
- Saunders, P.F., and Maxwell, S., 1983: Microfouling, macrofouling and corrosion of metal test specimens in seawater: *Microbial Corrosion*, The Metals Society, London, England, p. 74-83.
- Stroes-Gascoyne, S., 1989: The potential for microbial life in a Canadian high-level nuclear fuel waste disposal vault—A Nutrient and Energy Source Analysis: Atomic Energy of Canada, Limited Report #9574

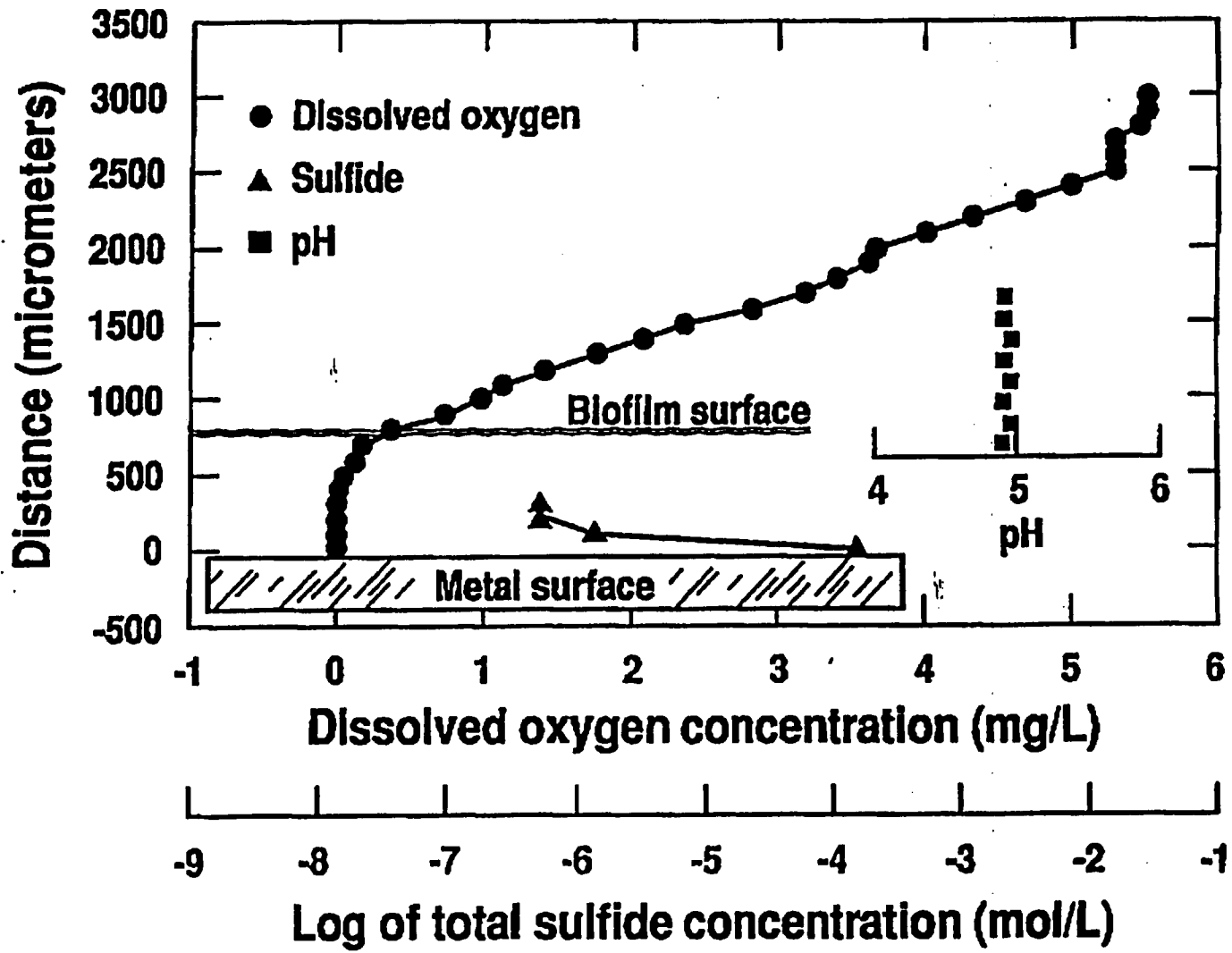


Figure BL-1 Strata within a typical biofilm and possible reactions within the strata

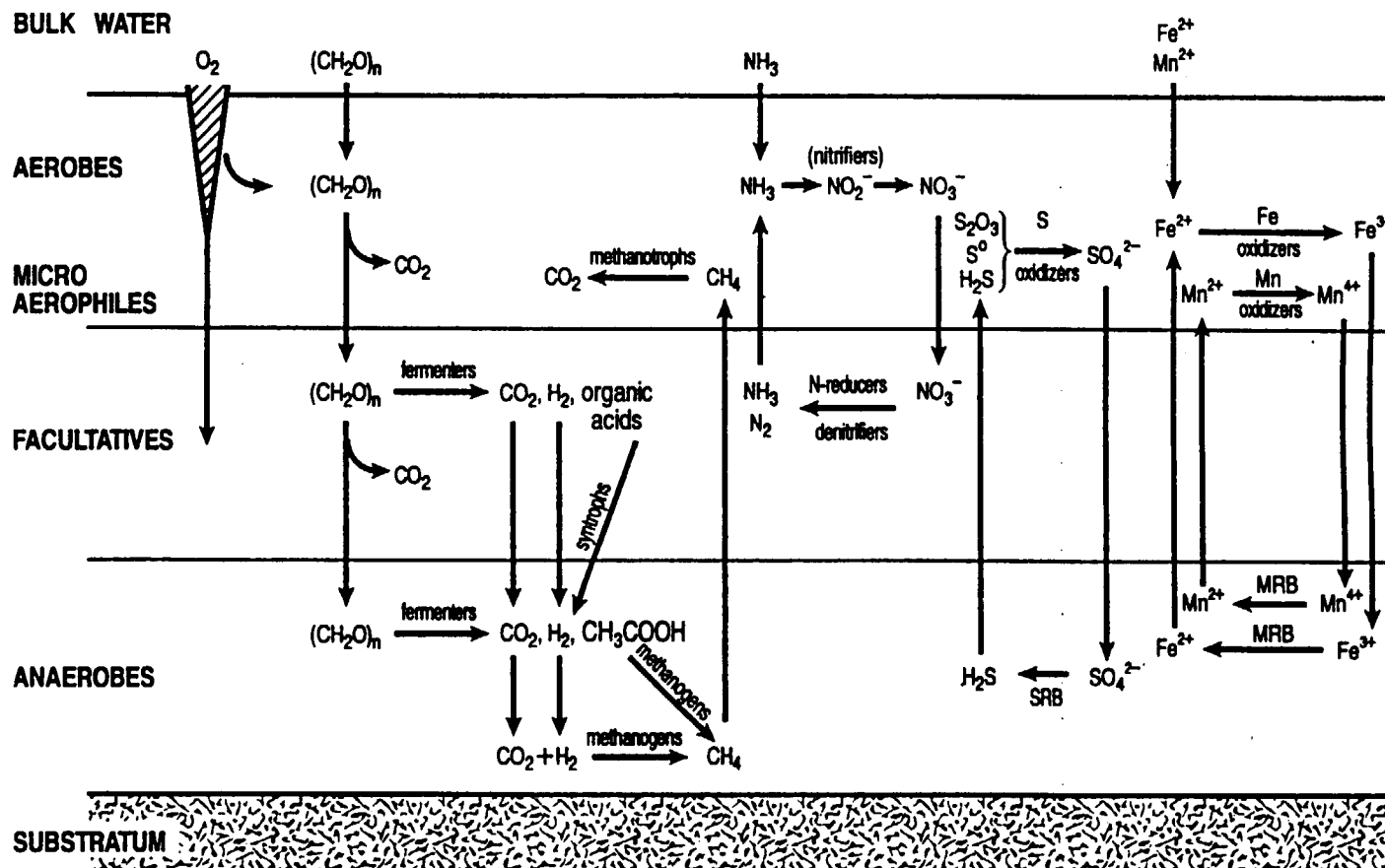


Figure BL-2 Concentration profiles of sulfide, oxygen, and pH in a biofilm on mild steel (from Little, Wagner, and Ledwadowski, in press)

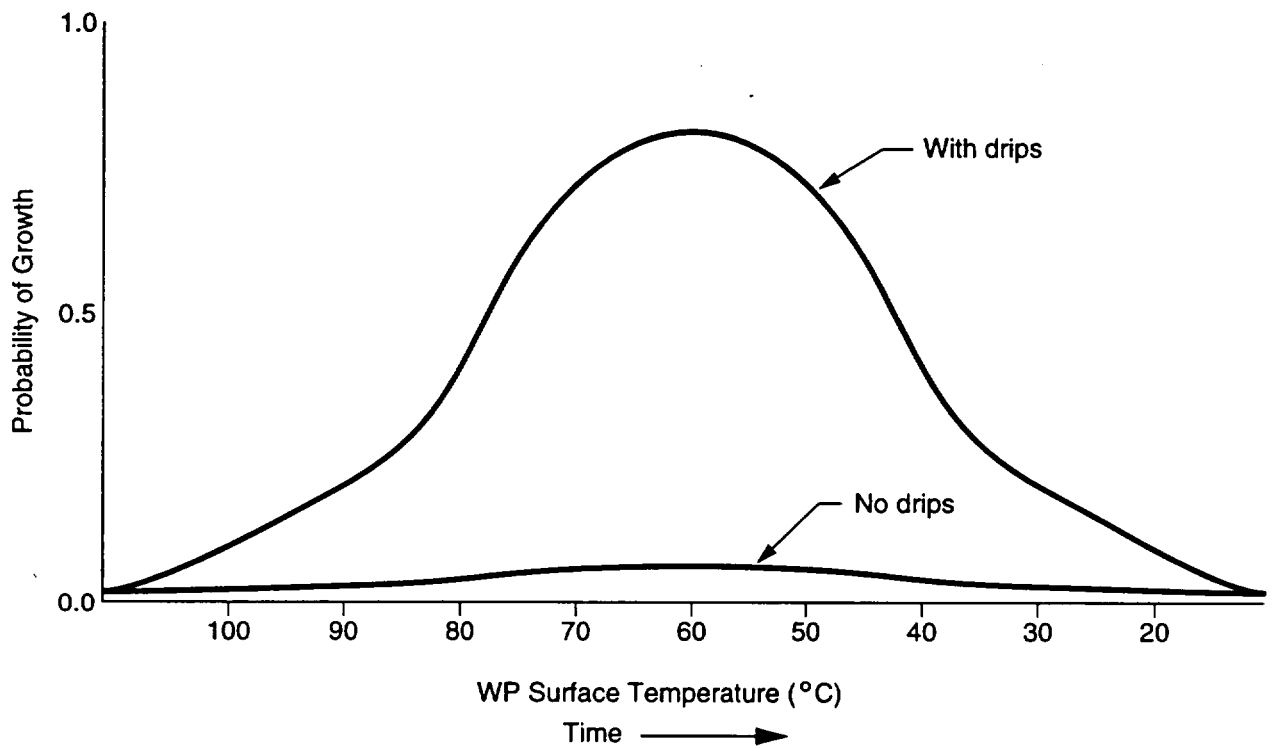


Figure BL-3 Relationship between the probability of growth of microbes as a function of waste package (WP) surface temperature. Note that because of waste package cooling, the decrease in temperature also represents increasing time

<i>Growth @ 60 deg C</i>	<i>Biofilm on CRM given Drips</i>	<i>Ennoblement</i>	<i>Alloy</i>	<i>Localized Corrosion</i>
--------------------------	-----------------------------------	--------------------	--------------	----------------------------

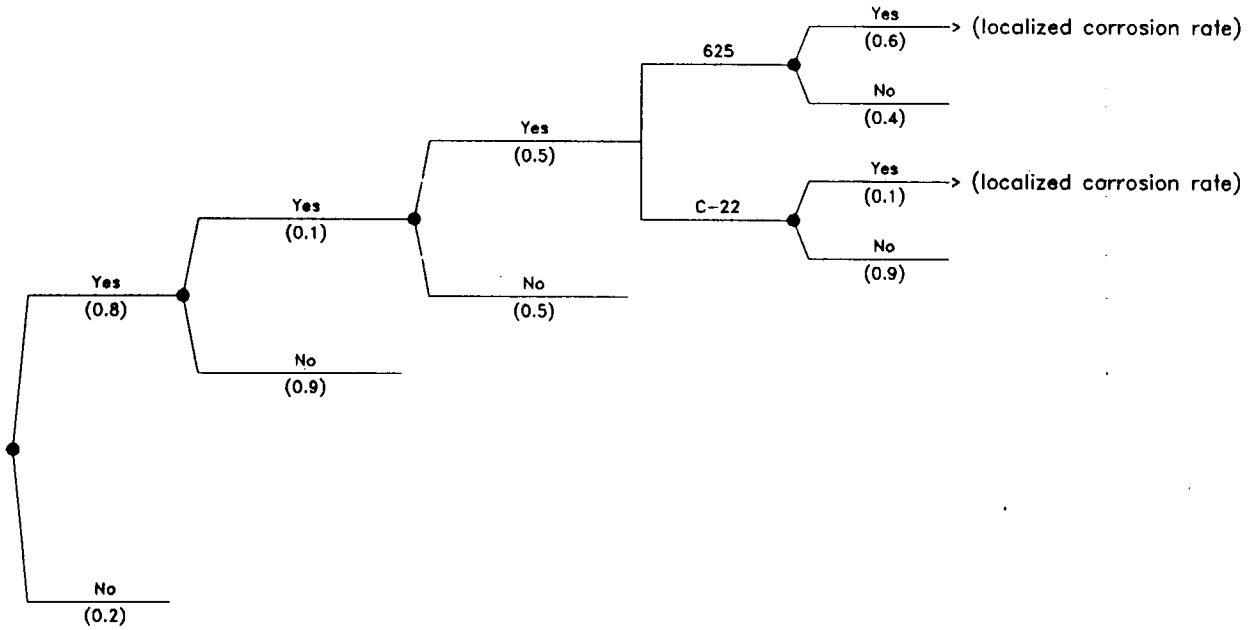


Figure BL-4 Logic tree showing possible influence of MIC on corrosion of CRM

<i>Development of Biofilm</i>	<i>Sulphide Production by SRBs</i>	<i>CAM</i>	<i>Localized Corrosion</i>
-------------------------------	------------------------------------	------------	----------------------------

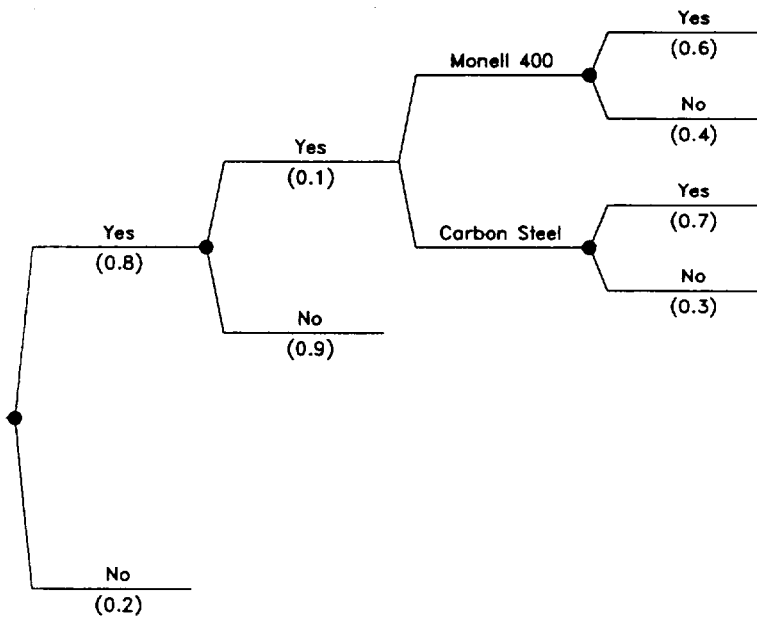


Figure BL-5 Logic tree showing relationship of MIC to corrosion of CAM

## ELICITATION SUMMARY

R. DANIEL McCRIGHT

### OVERVIEW OF WASTE PACKAGE CORROSION PROCESSES

The temperature and humidity conditions during the lifetime of the potential repository, as well their effects on the chemistries of the system, will define the mechanisms and rates of corrosion of the waste packages. The dry, hot period following emplacement of the waste packages will be characterized by low-temperature oxidation of the carbon steel outer barrier. This period will be typified by low rates of corrosion and development of crystalline and/or amorphous oxides. The only potentially significant occurrences during this period are low-probability "birth defects" such as undetected weld cracks that might propagate through the wall. If O<sub>2</sub> availability is low as a result of boiling, the iron will oxidize to lower oxidation states.

The oxides that form during this period will incorporate the dust and debris that fall on the waste packages. The oxide films will be thin because of the low temperatures, likely will be formed in a layered structure and will have kinetics that may be driven by the impurities and defects they contain. The expectation is that lower-valence oxide (Fe<sub>3</sub>O<sub>4</sub>) forms nearest the metal surface, with higher-valence oxide (Fe<sub>2</sub>O<sub>3</sub>) forming on top of the lower-valence oxide. In addition, Fe<sub>2</sub>O<sub>3</sub> is polymorphic, whereas the form most often observed in iron corrosion and oxidation I believe is FeOOH.

The concrete liner will decompose thermally and, assuming there is available CO<sub>2</sub>, will degrade through carbonation. As temperatures decrease, relative humidity increases, and the potential exists for dripping water, the concrete will react further. Because the concrete has abundant Ca, the pH will increase. Water passing through the concrete possibly will attain a pH of 9 to 10.

The presence or absence of drips, during all parts of the potential repository's lifetime, is important to degradation of both the outer corrosion-allowance material (CAM) and the inner corrosion-resistant material (CRM). The frequency and amount of dripping will control the amount of time the package stays wet. Drips during the hotter period will evaporate immediately when they contact the package surface, leaving behind salt deposits. As temperatures decline and the liner degrades, concrete will spall off as small particles and debris. Given the dust and concrete debris that will also fall on the packages and the oxide layer, the solutions that will form on the packages during dripping likely will be saturated with a number of constituents such as  $\text{CaCO}_3$ , calcium sulphate, Na, and K. Drips are the only mechanism that can create conditions that could cause localized corrosion of the inner barrier.

### **CORROSION OF CARBON STEEL OUTER BARRIER**

"Low"-temperature oxidation of the CAM will characterize the early hot, dry period of the repository. These temperatures are "low" relative to more than  $500^\circ\text{C}$ , at which significant oxidation of carbon steel has been observed. At high temperatures, the oxides form a thick, flaky film. However, at the lower temperatures expected for the repository, a thin film will form composed of crystalline, amorphous oxides. No significant flaking or spalling is expected.

Although a short period of oxygen sparging may occur related to boiling water (effectively creating a deaerated steam environment), I expect there to be sufficient oxygen even in a water vapor environment to develop iron oxides. The effect of the oxygen deficiency might be to oxidize the iron to lower oxidation states, such as  $\text{Fe}_3\text{O}_4$ . The oxide film will form with layering and will incorporate dust and other impurities. These impurities may be important to the reaction kinetics that occur later when humidities rise.

During the hot period ( $T > 100^\circ$  to  $150^\circ\text{C}$ ), boiling will make it unlikely that drips will occur in the repository. Any drips that do occur will fall on a very hot waste package, evaporate, and leave behind salt residue. Drips that pass through the concrete likely will be

concentrated J-13 water containing bicarbonate,  $\text{Na}^+$ ,  $\text{K}^+$ , etc., and will saturate with Ca because of the concrete. Because the concrete will degrade thermally and through carbonation with  $\text{CO}_2$  before it experiences drips, the pH of the water passing through it (about 9 to 10) will be lower than expected for new concrete (pH 12). In fact, it may be difficult to develop and maintain high pH conditions on the surface of the waste package.

The relative humidity (RH) thresholds between dry and humid air corrosion, and between humid air and aqueous conditions, is largely a function of the constituents. A clean carbon steel surface has a higher RH threshold than a surface containing oxides, dust, and evaporites related to drips. Gdowski found the critical RH threshold for carbon steel samples pretreated with salt solution to be about 65 percent (Gdowski, in press). The following RH thresholds for the dry-to-humid air transition and their associated uncertainties (expressed as a normal distribution within the range given) are estimated. For want of better information, I assume a normal distribution of values.

<u>Surface Condition</u>	<u>RH Threshold</u>	<u>Range in Uncertainty</u>
Oxides, salts, dust	65%	60% - 70% (normal distrib.)
Oxides, dust	75%	70% - 80%
Dust	85%	80% - 90%

The conditions expected on the waste packages will be oxides plus dust. Because of the period of dry oxidation, an oxide layer will be present everywhere except, perhaps, where it is has spalled. The presence of salts requires dripping conditions, and the volatile components are the most important (e.g.,  $\text{HCl}$ ,  $\text{HNO}_3$ ). The actual salts present may affect the RH thresholds.  $\text{Na Cl}$  will cause the threshold to be higher;  $\text{CaCl}_2$  will cause it to be lower. This effect is attributed primarily to the hygroscopic properties of the individual salts. Calcium chloride is more hygroscopic than is sodium chloride. In applying this RH threshold to the waste packages, I assume that those packages that experience drips will have salt deposits on their upper half (upper 180-degree angle in cross section). Those waste packages not experiencing drips are assumed to have only oxides on their surfaces.

The relative humidity threshold between humid air and aqueous conditions is also affected by oxides and salts on the surface. Further, I consider true aqueous conditions to be present only under dripping conditions and on the top and bottom of the waste package where water can accumulate. The "top" of the waste package is defined as the upper 60-degree angle; the "bottom" is the lower 60 degrees. The bottom is included because, after the pedestals have degraded, the waste package will lie on the invert, and dripping water that runs down the sides may accumulate at the bottom.

The following cumulative distribution function expresses my uncertainty in the RH threshold between humid air and aqueous conditions.

<u>Percentile of CDF</u>	<u>RH (oxides)</u>	<u>RH (oxides + salt)</u>
100%	100%	95%
90%	97%	90%
50%	95%	85%
10%	90%	80%
0%	85%	70%

Again, the effect of salts (expected in the dripping case) is to lower the RH threshold at which aqueous corrosion begins.

The assessment for the temperature threshold and its uncertainty for initiation of humid-air or aqueous corrosion is:

<u>Percentile of CDF</u>	<u>Temperature (°C)</u>
100%	105
50%	101
0%	97

The corrosion mechanism that occurs in the carbon steel is a function of pH. At a neutral pH of 4 to 9, general corrosion is expected; at pH 9 to 10, high-aspect-ratio pitting is expected. I

---

think it important to evaluate the probability that high pH conditions will occur. The concrete lining will have undergone significant thermal degradation and carbonation before dripping conditions are expected to occur. Further, the potential for maintaining high pH conditions on the surface of the waste package after drips have occurred should be considered. I suggest that there is a very low probability for a pH greater than 9.

The other possible problem is susceptibility to stress corrosion cracking (SCC) when the carbon steel begins to passivate, but the passivation is incomplete. Parkins, Uhlig, and others have done a lot of work on SCC susceptibility of carbon and alloy steels in hydroxide, nitrate, and carbonate environments. From the work to date, it is difficult to say whether carbon steel would suffer from SCC under Yucca Mountain conditions. As regards caustic-induced SCC, the repository probably would always have too low a pH for this to be a concern. However, carbonate- and nitrate-induced SCC appear to occur within rather specific environmental ranges, and in many of the reports in the literature are further induced by applied potential. The composition and microstructure of the steel also seem to play a role. Other chemical species in the water seem to act as inhibitors. Thus, I recommend an empirical approach to resolve this problem. Fortunately, we have started some SCC testing of carbon steels in environments relevant to the potential repository. Work being performed on concrete degradation in the repository will yield results on changes in water chemistry, information that will be incorporated into our SCC testing activities.

Given moderately alkaline pH conditions, the expected aspect ratios for pit formation may be high, but I don't have a good sense of the magnitude. The range of pH 9 to 10 represents a transition from active corrosion to passivation for the steel, so that the localized corrosion pattern is certain to be affected by other chemical species and other factors.

Elevated concentrations of  $\text{Cl}^-$  are required to develop high-aspect-ratio pits under alkaline conditions. Without a continued supply of  $\text{Cl}^-$  ions, carbon steel is repassivated. Initially, high concentration of  $\text{Cl}^-$  may be supplied by dripping water, but with continued dripping,  $\text{Cl}^-$  concentration will be reduced, thus decreasing the probability of maintaining the growth of high-aspect-ratio pits. It would be expected that chloride ion would promote pitting even in

alkaline environments, but chloride ion is not the dominant ion in J-13 water (nitrate ion, which is also present in J-13 water and at a comparable level to chloride, tends to mitigate pitting effects and the effects of the two ions may effectively cancel one another),

Given a pH of 4 to 9, the CAM will degrade through general corrosion. Rather than describing the process by a "pitting factor," I would use a "localization" or "roughness" factor to describe the local roughness or variability of the general corrosion front, expressed as the ratio of the localized depth to the average depth of the general corrosion front. I expect the roughness of the surface to decrease with time and depth, from a maximum of about 2 to about 1. The reason for the decrease with time is that all of the factors that lead to variability at the surface will lessen with time. For example, the local presence or absence of dust or debris and local variations in moisture may lead to variability of the initial corrosion front. These differences will decrease with depth and the development of corrosion products. In addition, oxygen will be progressively less available with depth as a thick layer of corrosion products develops, which may slow the general corrosion rate.

The corrosion localization or roughness factor is recalculated from some data on long-term corrosion rates acquired in the Southwell and Alexander work in the Panama Canal Zone (Southwell and Alexander, 1970). Specimens of a variety of materials were exposed to (1) fresh water at Gatun Lake, (2) sea water in the Pacific Ocean, and (3) conditions of mean tide elevation in the Pacific Ocean. Because the study was so extensive and systematic and the specimens were exposed for as long as 16 years, results from this study are cited frequently. We used their corrosion data for a low-carbon steel (0.25 C) after 1, 8, and 16 years of exposure. In this recalculation of their data, the average corrosion penetration is found by multiplying the measured average corrosion rate by the exposure time. The localization factor is found in one case by dividing the average pit depth (measured for the 20 deepest pits) by the average corrosion penetration at each exposure period. Similarly, in the second case, the localization factor is found by dividing the deepest pit depth by the average corrosion penetration.

**TABLE 1**  
**LOCALIZATION FACTORS CALCULATED FROM THE PANAMA CANAL ZONE STUDY DATA**

Environment	Surface Condition	Average Corrosion Penetration ( $\mu\text{m}$ )			Localization Factor Ratio of Average Pit Depth to Average Corrosion Penetration			Localization Factor Ratio of Deepest Pit Depth to Average Corrosion Penetration		
		Duration			Duration			Duration		
		1yr	8yr	16yr	1yr	8yr	16yr	1yr	8yr	16yr
Fresh-Water	Pickled	196	559	712	2.59	2.64	2.57	3.11	3.23	3.32
Immersion	Machined	191	508	635	2.93	3.00	2.60	3.46	4.40	3.76
	Millscale	160	482	635	4.61	2.53	2.64	6.35	3.90	3.64
Sea-Water	Pickled	150	661	1168	6.94	2.54	1.96	10.5	3.18	3.37
Immersion	Machined	140	686	1244	6.89	2.15	perf	11.6	5.81	perf
	Millscale	107	584	perf	13.1	perf	perf	24.7	perf	perf
Mean Tide	Pickled	241	584	1194	1.68	1.74	1.40	2.80	2.83	2.08
Conditions	Machined	279	635	1067	1.91	1.80	1.24	4.19	4.96	1.74
	Millscale	236	458	1118	1.94	2.50	1.23	2.58	3.50	2.32

Note:  
 Data originally from C.R. Southwell and A.L. Alexander, Materials Protection, Jan. 1970, p. 14, but taken from tables in the survey of degradation modes for iron-base, corrosion-allowance materials. D.W. Vinson, W.M. Nutt, and D.B. Bullen, UCRL-CR-1206464, June 1995 (Tables III-A, B, C, D).

Table 1 shows first of all that the localization factor varies considerably, and is highest for the most aggressive environment in this study, namely sea water. Several of the coupons (nominal 1/4-inch thickness) were perforated after 8 or 16 years of exposure to sea water. In nearly all cases, the localization factor decreased with time.

If we focus primarily on the data for corrosion in fresh water, which is more relevant to our J-13 geochemical water (since the chloride ion content is not the dominant ion in J-13 water), the group of localization factors calculated from the average pit depth show a rather compact range—2.6 to 4.6. Based on the deepest pit depth, the ratios are somewhat higher, 3.1 to 6.4. Also note that in fresh water, the corrosion rate decreased rather markedly between 8 and 16 years, so that the average corrosion penetration did not increase greatly in this interval. By contrast, the corrosion rate slowed less in the sea water and mean tide exposures, so that the corrosion penetration was high after 16 years even though the localization factors tended to decrease with time. As might be expected, the localization factors achieved some high values in sea water—factors of 10 to 20 (and more).

I have done a similar analysis on another group of long-term corrosion data to estimate a localization factor. In this case, conditions were two different atmospheric exposures in humid climates. Both exposures used a series of very low-carbon, low-phosphorus steels with small additions of copper (these most closely resemble the “plain carbon steel” in the Southwell and Alexander survey).

**TABLE 2**  
**CORROSION LOCALIZATION FACTORS FOR ATMOSPHERIC EXPOSURE OF STEEL SPECIMENS**

Material (Refer to the original works for identification) All are low-carbon, low-phosphorus steels	Block Island, RI Exposure (marine atmosphere) after 9.1 years	Bayonne, NJ Exposure (industrial atmosphere) after 9.1 years	Bayonne, NJ Exposure after 18.1 years
41	2.35	2.86	1.69
43	2.47	2.76	2.22
64	2.87	2.74	2.25
40	2.42	2.96	2.29
58	2.36	2.92	2.20
42	2.45	3.31	2.10

See Tables II-I, J, K, and L in D.W. Vinson, W.M. Nutt, and D.B. Bullen, UCRL-CR-1206464, June 1995. Original data from a series of papers by Copson. The pitting factors were derived from measurements of the average of the four deepest pits on the top of the specimen and the average of the four deepest pits on the bottom.

Again, note that the localization factor tends to decrease with exposure time. Despite the differences in location and atmospheric conditions, the localization factors fall into a similar range. From the preponderance of information, and it appears that localization factors of 2 to 3 would cover most situations (like the 90th percentile in a cumulative distribution function). If for the time being we discard the Panama Canal sea water immersion data, the range of localization factors (for both the Southwell and Alexander and the Copson studies fall between 1.7 and 6.3, so this would represent the 100% cumulative distribution function.

In trying to apply this analysis to the repository setting, it appears that the localization factor would decrease with time and approach something just over 2, pretty much regardless of chemistry. It also appears that localization of the attack will always be a factor, in other words the corrosion is not completely uniform. Note also that the localization factors on the order of 2 are consistent with a "pitting aspect ratios" where the pit depth and width are of comparable dimensions. All of the exposure conditions have been at ambient temperature. We have no comparable information at higher temperatures, but the suggestion from the data gathered to date is that temperature probably is not a strong factor. The long-term corrosion

testing now underway eventually will provide information on localized corrosion of carbon steels at higher temperatures.

### **ALTERNATIVE CORROSION-ALLOWANCE MATERIAL**

Monel 400 is the alternative corrosion-allowance material. The corrosion rates for this alloy are less than for carbon steel. Based on 16-year Panama Canal data (Southwell and Alexander, 1970), the general corrosion rate is 61x less than that of carbon steel, and the pitting rate is 5x less. Like carbon steel, Monel 400 does not develop deep pits. Instead of having  $Fe^{+3}$  ions available from the carbon steel, cupric ions ( $Cu^{+2}$ ) will be available, which are less subject to less acidic hydrolysis than  $Fe^{+3}$ . Sulphate-reducing bacteria tend to cause dealloying of Monel 400. Under all of the expected conditions in the potential repository, Monel 400 would be expected to perform better than carbon steel. An issue is whether the improved performance is worth the additional expense. We did a degradation mode survey on Monel 400, relevant to its projected performance under Yucca Mountain repository conditions. We concluded that the material could perform as an "intermediate material," providing performance between that of the corrosion-allowance materials (such as carbon steel) and the highly corrosion-resistant materials (such as Alloy C-22). We have added Monel 400 to our testing program. As an outer barrier, it would function as a rather "resistant" corrosion-allowance material, and perhaps could be used in thinner section than the 10 cm proposed in the current design for carbon steel as the outer barrier material. (See Vinson and Bullen, 1995, for more corrosion data on Monel 400.)

### **CORROSION OF CORROSION-RESISTANT INNER BARRIER**

Depending on the corrosion mechanism of the CAM (general corrosion or pitting), the CRM gradually will be exposed. A potential benefit of the coupling of the inner and outer barriers will be galvanic protection that can slow the attack on the CRM. The effectiveness of galvanic protection is a function of the throwing power of the solution that contacts the metal couple, which, in turn, is dictated by the electrolyte conductivity. Given the expected electrolyte conditions in the carbon steel corrosion products, the throwing power will be no

---

more than a few centimeters. Assuming a neutral pH of 4 to 9, which is the expected condition across most of the waste packages, the carbon steel will undergo general corrosion. As the corrosion front intersects the inner barrier, large parts of the CRM will be exposed at nearly the same time. Thus, galvanic coupling will not provide much protection across the large openings in the CAM. Assuming a high pH of 9 to 10, which may result from drips that have traveled through the concrete liner, high-aspect-ratio pits may develop. As these pits intersect the CRM, galvanic protection would be more effective. The pits developed in carbon steel under high pH conditions are nearly spherical, having a narrow mouth and aspect ratios that generally do not exceed about 2. Therefore, even under high pH conditions, the time during which galvanic protection is operative likely will be limited.

In the present design, which calls for a 90-percent contact between the inner and outer barriers, there is a narrow crevice that may allow for moisture to enter and move along the gap. In addition, there may be residual thermal stresses due to the shrink-fit procedure that is planned. These stresses may lead to stress corrosion cracking of the CRM. Perhaps, because the potential for effective galvanic protection is short-lived, a larger gap between the inner and outer barriers should be considered.

Following the relatively brief period of galvanic protection, exposure of the CRM will begin. There are limited experimental data to evaluate the corrosion mechanisms and rates for the candidate CRM materials under expected environmental conditions. Only very slow general corrosion, not pitting or crevice corrosion, is expected under these bulk environmental conditions. Most of the corrosion experiments are conducted under harsh conditions of pH,  $\text{Cl}^-$ , temperature, and  $\text{O}_2$  in short-term tests (from a few hours to a few days). For example, plots have been developed for 300 stainless steel between  $\text{Cl}^-$  and pH,  $\text{O}_2$ , and temperature. Boundaries can be identified that separate fields (combinations of conditions) of attack and no attack. If such plots existed for the candidate CRM materials such as C-22 and 625, the expected environmental conditions would lie in the "no attack" fields. Perhaps the uncertainty in the position of the boundaries could be incorporated and used to assess the probability that localized attack could initiate with these alloys.

The only mechanism for elevated Cl<sup>-</sup> concentrations is dripping water, and the only mechanism for low pH is within a crevice. Therefore, I conclude that there will be no localized corrosion of the CRM without dripping water. Otherwise, general corrosion will occur. General corrosion rates for these materials usually are low under most aqueous conditions. For example, average general corrosion rates (with no pitting or crevicing) are reported on the order of 1 to 3 micrometers/year for Alloy 825 in sea water. As a rule of thumb, general corrosion rates double for each 30°C rise in temperature; even in the 60° to 100°C range, the highest rates might be only 4 to 12 micrometers/year. From what I have seen, these rates tend to be steady with time. We soon will acquire general corrosion data on the CRM from our long-term test facility, where weight-loss coupons have been exposed for six months to simulated 10x J-13 water, simulated 1000x J-13 water, and acidified (pH ~2.7) J-13 water. These tests will continue.

Some years ago, we did some corrosion testing in actual (as opposed to simulated) J-13 well water. Specimens of Alloy 825 (and other materials --primarily 300 austenitic stainless steels, then the focus of our work) were immersed in the water at different temperatures and other relevant environments. Results are given in the following table.

CORROSION RATES OF ALLOY 825

Temperature (°C)	50	80	100	100	150
Environment	J-13 well water	J-13 well water	J-13 well water	Saturated vapor above J-13 well water	Atmospheric gases and water vapor (not pressurized)
General Corrosion Rate (µm/yr)	0.211	0.109	0.049	0.030	0.030

The corrosion rates, determined from the weight loss, represent the average of three replicate specimens in each temperature/environment condition. The water immersion and saturated vapor specimens were exposed for 10 to 11,000 hours (over a year), while the 150°C

atmospheric exposure lasted 3800 hours. One would expect Ni-Cr-Mo alloys to show similar if not lower corrosion rates. This work indicates that in the absence of localized corrosion, the corrosion rates (wet or dry) are small enough that the inner barrier would last an exceedingly long time. It is interesting to note that under immersion conditions, the corrosion rate decreases at higher temperature, probably because of the lower oxygen solubility (McCright et al., 1987).

Given bulk environmental conditions of dripping water; temperatures 80° to 30°, decreasing with time; pH 4 to 9 with some probability of high pH conditions; and concentrated J-13 water from salts in solution, there is a finite, but small, probability that localized (crevice) corrosion of the CRM will initiate. For illustration, assume that 1000 waste packages experience these conditions. Figure DM-1 illustrates my assessment of the number of packages out of this 1000 that might initiate localized corrosion as a function of time. Time, in this case, begins after temperatures have cooled to about 80°C. Temperatures will decrease with time, as will Cl<sup>-</sup>. As a sensitivity check, the numbers given in Figure DM-1 can be compared with the results when the actual number of packages that will experience drips is assessed (by the hydrologists) and assuming that, given drips, there is a probability of 1.0 that localized corrosion will occur.

Given that localized corrosion initiates, the rate of growth or penetration can be described by a growth law having the form:

$$p = Kt^n$$

where  $p$  is the penetration rate,  $t$  is time since initiation, and  $K$  and  $n$  are constants related to the manner in which the rate varies as a function of time and environmental conditions. For both alloys C-22 and 625, my best estimate of the value of  $n$  is 0.4. I express the uncertainty in this estimate with a normal distribution centered on 0.4, having two-standard deviation (2) values of 0.3 and 0.5, and lower and upper limits of 0.2 and 0.65. This estimate is based on analogies with other materials (primarily austenitic stainless steels). Still, it is important to emphasize that it is difficult to initiate pitting on these very corrosion-resistant materials; one

must use "extreme" environments and/or high applied anodic potentials to produce discernible pits.

A phenomenological expression for K in terms of chemical speciation would be of the following form with terms for temperature, hydrogen ion concentration, chloride ion concentration. Other species in the solution would also be a factor, but the analysis quickly becomes more complex since some ions (like nitrate) impede pitting.

$$K = K_0 \exp(-Q/RT) [H^+]^a [Cl^-]^b \dots$$

where Q is the activation energy. Evaluation of these terms would be alloy specific. I will leave it to other panel members who are much more knowledgeable about pitting to provide an evaluation of the terms.

Once pits have initiated, there is a trade-off between the number of pits that can continue to grow and the depth that pits can attain. Cathodic current is the limiting factor, and a balance must be maintained between cathodes and anodes. Either some pits are stifled so that a few pits can continue to deepen, or larger numbers of shallow pits are maintained.

## **MICROBIOLOGICALLY INFLUENCED CORROSION**

As temperatures continue to fall and relative humidity rises, the potential for microbiologically influenced corrosion will occur. At temperatures less than 100°C and relative humidities of 60 to 70 percent, various fungi and bacteria will grow. Fungi can grow at an RH of 60 percent, but require organic carbon. According to a colleague who specializes in microbiology, fungi are saprophytic organisms that require organic sources of carbon. Given the limited amount of organic carbon expected in the repository, it appears that MIC effects likewise will be limited. MIC is one condition that might lower pH over time. This could have a large effect on the corrosion rates for the carbon steel, but at least some of the CRM materials appear to be immune. MIC will be controlled by the availability of water and nutrients, which are both in limited supply.

## OTHER ISSUES

### Welds

The current plan is that all assembly welds will be annealed at high temperatures, which will homogenize the structure. The small residual stresses or cracked welds that escape detection may be one cause of the initiation of localized corrosion of the CRM. Welding of the CRM may leave it somewhat more brittle, depending on the microstructure that is produced. Addition of molybdenum is beneficial to improving the resistance of stainless steels and nickel-base alloys, but certain Mo-rich (and Cr-rich) phases (sigma, chi, mu and so on) are quite brittle compared to the gamma phase. The composition of the commercial alloys are 'balanced' between corrosion resistance and weldability issues, but in most cases it is important to adhere to the manufacturer's recommended heat treatment and welding practices throughout the container fabrication process to avoid detrimental microstructures. We are concerned, too, about phase changes that may occur over long periods of time at modest temperatures while the waste package is experiencing the thermal spike, and we have begun some long term aging studies to resolve whether this is a problem or not. We are also working with the nickel industry, since the manufacturers have a wealth of information in this area, and quite often small 'nuances' in composition and heat treatment can have a profound effect on formation on phase stability.

The closure weld may leave stresses if it is not annealed. Annealing the closure weld presents some difficulties if we are concerned about applying too much heat to the spent fuel cladding. Perhaps some MIC will localize at the welds, especially on carbon steel and perhaps on Alloy 400 (if it is used as the outer barrier). Welded carbon steel and CRM could be more susceptible to localized corrosion than the base material, because the varying microstructure in the fusion zone and in the heat-affected zone may contain a susceptible microstructure. Without detailed knowledge of the microstructures that will be present (which will depend on the welding practices), it is impossible to predict. However, one important point is that current manufacture of the high-performance Ni-Cr-Mo alloys specifies very low levels of carbon, sulfur, and phosphorus, which usually are the

troublesome elements in these alloys. The low levels of these elements mitigates many of the localized corrosion (pitting and intergranular) effects.

Thus, although welded regions for most metals are often the more corrosion-prone areas, low interstitial content, good welding practices, and good quality control may provide important offsetting factors. However, welded material will form a good fraction of the total surface area. At a workshop I attended at the Nickel Development Institute in 1995, it was pointed out that by current melting practices, it would take three ingots of material to make a single inner barrier container. This means a number of assembly welds, all of which in principle can be annealed. However, given the number of waste packages that will be produced and the number of assembly welds, this ends up being miles of welds, so that even with the best practices, it seems that somewhere a susceptible microstructure will be created. Right now, I think we know too little to identify the susceptible microstructure.

### **Ceramic Coating**

A ceramic coating placed on the outside of the waste package would be vulnerable to cracking and spalling from external impacts. By the time it is needed (when RH has increased in the repository), a partly cracked or spalled coating may not provide sufficient protection. Another issue is whether the ceramic coating will have low porosity and that what porosity it has is not interconnected. However, I have learned from colleagues that high density coatings can be produced, and since the coating is applied in multiple layers, interconnected porosity concerns are greatly reduced. There is obviously some skepticism about the feasibility of routinely producing high-integrity ceramic coatings and their mechanical survivability for long times in the repository. In a sense, comparison of the all-metal container with a ceramic coated container is the long term chemical stability of the metal versus the mechanical/structural issues with the ceramic. The Project is pursuing studies to determine the feasibility of a ceramic coating as a barrier and how such a coating would be configured - a coating on the outside of the CAM, on the inside of the CAM, or to coat the outside of the inside barrier, the CRM, making the coating less susceptible to cracking during handling and from contact with debris and the pedestals. It is premature to judge until these feasibility studies are completed.

### **Rare or Time-Dependent Processes**

Because of the long periods involved and the large number of waste packages, the potential exists for very rare or long-term processes to affect the degradation of the waste packages. For example, "birth defects," such as weld cracks that escape detection, are a possibility. This is primarily a quality control issue. Embrittlement due to phase changes or changes in microstructure over long periods is another possibility, and this was discussed in the section on welds since the welded area appears to be the most likely area for changes to occur. The performance assessment should include premature failure scenarios.

### **REFERENCES**

- Gdowski, in press, Revision 1 of Volume 3 of the Engineered Materials Characterization Report. The draft was distributed to the Expert Elicitation Panel Members in March, 1977. When it is published it will be UCRL-ID-119564.
- McCright, R.D., Halsey, W., and Van Konynenburg, R.A, 1987, UCID 21044, December.
- Southwell, C.R., and Alexander, A.L., 1970, Materials Protection, p. 14, January.
- Vinson, D.W., Nutt, W.M., and Bullen, D.B., 1995, UCRL-CR-1206464, June.
- Vinson, D.W., and Bullen, D.B., 1995, Survey of Degradation Modes of Cu-Ni Alloys, UCRL-122862, September.

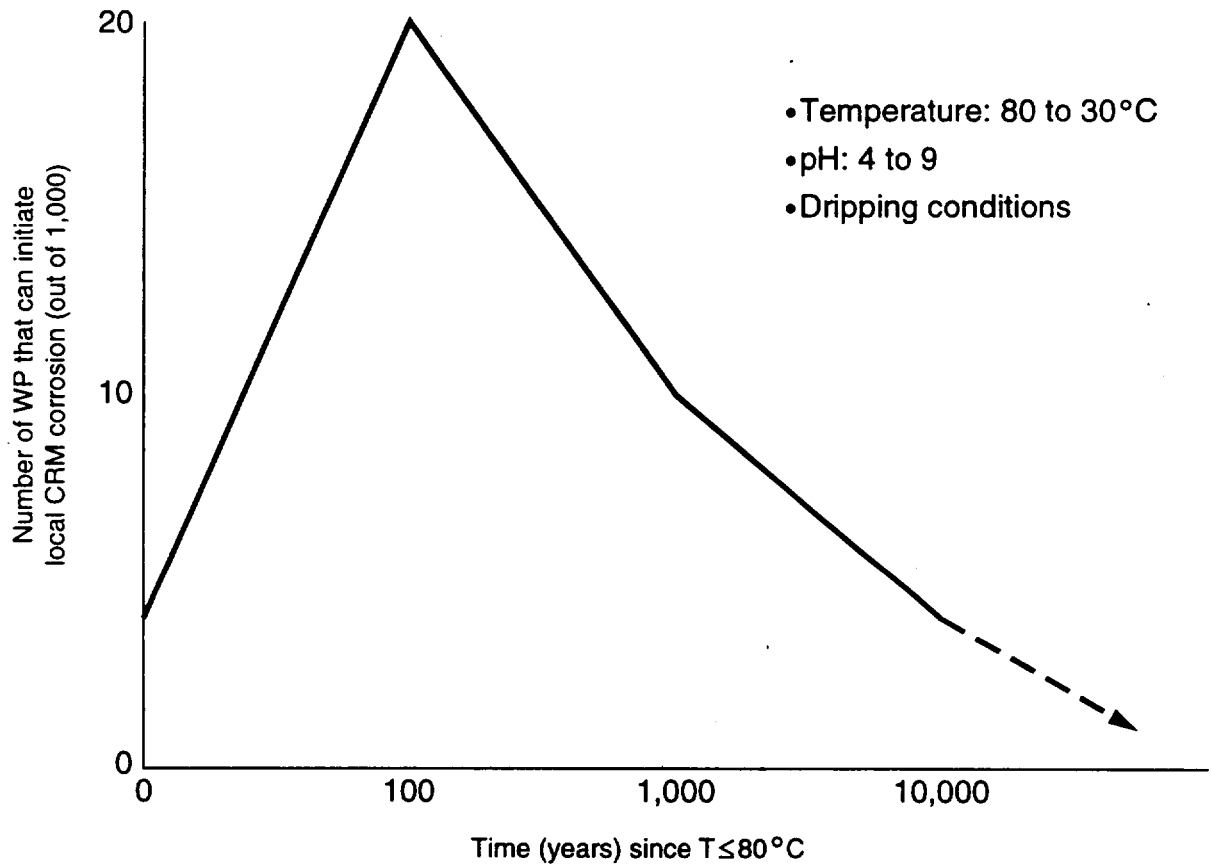


Figure DM-1 Schematic diagram showing the number (out of 1,000) of waste packages (WP) that are expected to initiate localized corrosion of the corrosion resistant package (CRM), as a function of time since temperature decline below 80°C

---

## ELICITATION SUMMARY

JOHN R. SCULLY

### OVERVIEW OF WASTE PACKAGE CORROSION PROCESSES

The time-evolution of environmental conditions within the potential repository will dictate the dominant corrosion modes, rates, and processes. During the early period, characterized by high temperature and low relative humidity, the dominant corrosion mechanism of the carbon steel corrosion-allowance material (CAM) will be dry oxidation. Oxygen partial pressures, CAM surface temperatures, and water partial pressures will control the corrosion processes at this time. Atmospheric gas may be excluded because of the large increase in volume of liquid water as it is converted to the vapor phase. However, the reaction of Fe with water vapor in the absence of O<sub>2</sub> is a spontaneous thermodynamic process that produces nonprotective FeO or Fe(OH)<sub>2</sub><sup>1</sup> (Davies et al., 1951; Davies et al., 1954).

The rates of these reactions in anoxic water vapor (at low relative humidities but temperatures greater than 100°C) should be obtained by experiment or literature evaluation. Unfortunately, most studies of Fe oxidation in steam have been conducted at higher temperatures than expected in the potential repository. Moreover, most studies are based on

---

<sup>1</sup> One possible thermodynamically favorable reaction in water vapor is  $\text{Fe} + \text{H}_2\text{O} = \text{FeO} + \text{H}_2$ . Wustite (FeO) is instable at low temperatures and may transform to Fe<sub>3</sub>O<sub>4</sub> via the reaction  $4\text{FeO} = \text{Fe}_3\text{O}_4 + \text{Fe}$  (Gulbransen et al., 1950). It should be noted that most so-called dry oxidation studies inadvertently include uncontrolled amounts of water vapor. Therefore, the influence of water vapor on so-called dry oxidation generally is unknown. It is possible that O<sub>2</sub> exclusion limits oxidation in the presence of intermediate or low relative humidities. Perhaps tenacious oxides of low thickness result. However, credit should not be taken for a period of low oxidation unless substantiated by experiments in water vapor at low partial pressures of oxygen and at temperatures from 100° to 200°C.

short-term lab tests that rely on mass gain to quantify oxidation rates; data are lacking for lower temperatures where lower rates of mass gain require either longer exposures or more sensitive detection methods to adequately define rate laws that can be applied to periods of 100 to 1000 years (e.g., surface science methods)<sup>2</sup>. Once the temperature decreases to near 100°C, or if back-diffusion of O<sub>2</sub> is faster than convection produced by evaporation of boiling water even at higher temperatures, dry oxidation will occur in the presence of increasing partial pressures of O<sub>2</sub>. Graham reports that oxidation of Fe is logarithmic below 200°C and parabolic above this temperature (Graham et al., 1970). Therefore, over extremely long periods, it is reasoned that the slow, dry oxidation process will give rise to the thickening of a relatively brittle corrosion product that because of stress accumulation eventually is susceptible to spalling. Episodic wetting/ drying cycles contribute to the propensity for spalling. The Billing-Bedworth ratio and oxide growth epitaxiality govern spalling versus porosity of corrosion product. Depending on the amount of spalling that occurs, the increase in relative humidity with time will lead to either capillary condensation onto a thick oxide layer before humid-air corrosion of the CAM begins, or, in the case of much spalling, the immediate initiation of humid-air corrosion of steel covered with a thin, dry layer of oxidation.

As temperature decreases and relative humidity increases following the hot, dry period, water will begin to adhere to and link sites on the carbon steel and oxide layer. Availability of dissolved oxygen is related to thickness of water film and partial pressure of atmospheric oxygen (Henry's law). Moisture will go from being at local sites, to islands, to monolayers, to pools or layers of bulk water, depending on relative humidity, temperature, and surface curvature. Humid-air corrosion relative humidity thresholds depend critically on the presence of hygroscopic salts from prior dripping wetting/drying sequences.

---

<sup>2</sup> This situation is analogous to that of stress corrosion cracking, for which "windows" of slow crack growth have not been explored as thoroughly as regions of rapid crack growth because of the difficulty of the experiments and the experimental patience required.

Electrochemical processes begin when more than several monolayers of water have developed. At this point,  $\text{Fe} \rightarrow \text{Fe}^{2+} + 2e^-$  (metal dissolution—anodic reaction) and  $2\text{H}^+(aq) + 1/2\text{O}_2(aq) + 2e^- = \text{H}_2\text{O}(l)$  (reduction of dissolved oxygen—cathodic reaction) reactions begin. To understand the relative importance of the thickness of the water film, the following shows the potential effect that variations in pH, oxygen partial pressure (or oxygen solubility), and microbiologically influenced corrosion (MIC) can have on the corrosion rates of the CAM.

#### Potential Effect on Aqueous Corrosion Rate

Acidic pH	Factors of 100 to 1000
Oxygen partial pressure (or oxygen solubility)	Factors of 10 to 100
MIC	Factors of 1 to 6

Thickness of water film is governed by the relative humidity, temperature, hygroscopic salt identity, and capillary radius. In “humid-air” conditions, film thickness is on the order of micrometers; to approach bulk “aqueous” conditions, it must be on the order of 100 micrometers or greater. As temperature decreases in the repository and relative humidity increases, humid-air corrosion mechanisms will be dominant. At some locations, dripping conditions may occur, which will lead to aqueous corrosion mechanisms. For the potential repository, it is important to understand the potential for dripping conditions and their frequency, because this may lead to wetting/drying and concentration of salts. Salt caking may cause the aqueous conditions to remain longer on the surface of the waste package.

Assuming relatively neutral pH conditions ( $4 \leq \text{pH} \leq 10$ ), the corrosion of the CAM will occur primarily through the advancement of a general corrosion front. By definition, “pits” require separation of anode (active pit site) and cathode (passive surfaces), a process that is not expected to occur for carbon steel under neutral or acidic conditions. Rather, hemispherical “craters” will form that coalesce with depth and time to form a relatively uniform corrosion front. The driving force for corrosion of steel in neutral aqueous waters is

oxygen reduction following its mass transport through a water film to the steel interface. If this process governs corrosion of the steel at this stage, then “ridges” between craters would tend to be leveled with time. If pH conditions are relatively high (pH  $\geq 9$  to 10) because drips of water pass through the concrete liner, high-aspect-ratio halide-induced pits and crevices may form in the CAM, because the steel will be passivated at its open-circuit potential and exhibit low passive-current densities. It should be noted that there are reported instances of pitting of steel at neutral pH levels, but two factors need to be considered. First, the passivation potential increases considerably with lower pH: spontaneous passivation becomes less likely at the aerated steel open-circuit potential, and passive current densities become orders of magnitude higher than observed at pH  $> 9$  (Pourbaix, 1974). These factors make it difficult to form high-aspect-ratio pits. Second, some instances of “pitting” at neutral pH are examples of shallow cratering or surface roughening governed by other factors; these effects are not the same as high-aspect-ratio pitting observed on materials that form strong passive films.

To describe the rate of pit growth in the CAM under high-pH aqueous conditions, pit growth laws can be defined that are a function of the chloride (Cl) content, temperature, electrochemical potential, and O<sub>2</sub> availability. In addition, the spatial density of growing pits can be assessed as a function of pit depth. As depth increases, the number of growing pits decreases because of the limited cathode area available to support the increasing anode area produced by the growing pits. This decrease in density of growing pits is a reflection of the stifling of pits with depth (or time).

After CAM pits or general corrosion sites penetrate the outer liner, a short period of galvanic suppression of CRM corrosion begins that will be a function of the type of corrosion morphology related to the CAM. However, the possibility of Fe<sup>+3</sup> generation increases after all the CAM is converted to Fe<sub>2</sub>O<sub>3</sub>, FeOOH, and Fe<sub>3</sub>O<sub>4</sub>. The presence of Fe<sup>+3</sup> without galvanic suppression is detrimental to the CRM, in that Fe<sup>+3</sup> promotes localized corrosion processes on Ni-Cr-Mo-Fe alloys because of its role as an oxidizer.

As for the CAM, we can describe the growth of pits within the corrosion-resistant material (CRM) inner barrier. In this case, few experimental data are available to define empirically the growth laws in Ni-Cr-Mo-Fe superalloys and, until additional experimental data are available for the candidate materials (alloys 625, Hastelloy C-276, and C-22), there are large uncertainties. However, the threshold salinity [ratio of halides/other anions], electrochemical potentials, and temperatures for susceptibility of these alloys are much greater than for the CAM steel. Moreover, the susceptibility of these alloys to pitting and crevice corrosion is a strong function of temperature (see below). As the surface of the waste package cools, these alloys might enter defendable windows of immunity from localized corrosion processes.

#### **CORROSION OF CARBON STEEL OUTER BARRIER**

During the early period, when conditions in the potential repository are relatively hot and relative humidity is low, corrosion of the outer barrier will occur through a combination of dry oxidation or corrosion in water vapor with a low partial pressure of oxygen. Oxygen partial pressures and temperature will control the rate of oxidation. It is possible that oxygen sparging due to boiling of water will lead to very low partial pressures, but this remains to be verified. Dry oxidation produces a brittle corrosion product that is susceptible to spalling. The critical depth of the oxidation layer at which spalling can occur is a function of temperature and oxygen partial pressure. At low temperatures and low partial pressures, spalling will be less likely than at higher temperatures and partial pressures. However, we lack evidence of spalling at low temperatures and pressures based only on relatively short-term data. My recommendation is that the critical factors controlling spalling (e.g., oxide thickness, epitaxiality) be defined and that growth laws be defined for conditions of low temperature/low O<sub>2</sub> partial pressure. In combination, these data should reveal whether spalling occurs in the first 100 to 1000 years when temperatures are high, relative humidities are low, and O<sub>2</sub> exclusion may occur. For relative humidities less than 60 percent, my conservative assessment of the relative likelihood of low, moderate, or high spalling potential is: low (0.1), moderate (0.6), and high (0.3). This expresses my uncertainty in the degree of spalling. The spatial variability on various waste packages or on the surface of a single waste package likely would be limited (assuming equal temperatures and oxygen partial pressures).

The basis for this assessment is limited research on thermal oxide scales on steel, review of the literature, and the position that "saving graces" such as low dry oxidation rates should not be assumed.

The presence or absence of spalling and the degree of spalling, in turn, affects the threshold relative humidity at which humid-air corrosion of the CAM begins. If there is no spalling, a relatively thick oxide layer will form so that capillary condensation will occur, but a thick, non-porous oxide layer would resist humid-air and aqueous corrosion. If there is moderate spalling, then capillary condensation will occur at cracks in the oxide, setting up aqueous corrosion more readily at these sites, but there will also be local humid-air corrosion. As a result, the threshold relative humidity will be somewhat less at oxide cracks than for the unspalled surface. Finally, with high spalling, much of the carbon steel will be exposed, and humid-air corrosion will begin at relative humidities comparable to those observed for carbon steel that has not been thermally oxidized. I use aqueous corrosion to define corrosion in bulk waters.

To a large degree, the areas of spalling of the oxide layer serve to localize subsequent humid-air corrosion. As discussed later, the initiation of pits (given high pH) is judged to be slightly more related to spalled areas, and the density of growing pits is also related to whether spalling has occurred. Therefore, the oxidation processes that occur during the dry oxidation period set up conditions on the waste package that can influence subsequent humid-air and aqueous corrosion.

The presence of drips will have a pronounced effect on the corrosion of the carbon steel outer barrier. It is assumed that there will be few drips during the early dry and hot period, because of a boiling/evaporation front in the rock farther from the canisters. Drips that occur will lead to concentrated chemistries as water boils and evaporates. As temperatures decrease to about 100°C and relative humidities increase to about 50 percent, more drips will reach the canisters and will evaporate immediately, leaving salt deposits. At low relative humidities, it can be assumed that the conditions are humid-air conditions; however, at higher relative humidities (95 percent), the drips could lead to alternating aqueous and humid-air conditions.

---

Hygroscopic salt caking will tend to maintain the aqueous condition on the waste package. Assuming that drips occur, the upper surface (upper 120° in cross section<sup>3</sup>) of the waste package will be affected by the drips (assume aqueous corrosion at relative humidities greater than 95 percent) and the side and bottom will remain in humid-air conditions, assuming high relative humidities. Dripping water might also accumulate at sites between package supports and the canister and under the canister after the supports deteriorate. Humid-air corrosion would be expected to occur over all surfaces that do not experience drips.

The pH conditions of the water that contacts the waste package will govern the mode of corrosion of the CAM. After the potential repository has cooled to below the boiling point, and relative humidities exceed the threshold for humid-air corrosion, drips may pass through the concrete liner. These drips, which would be expected to have an elevated pH of more than 9 to 10, would contact the upper surface of the waste package. At the same time, water films on the sides and bottom of the waste package and on those waste packages not experiencing drips would have neutral pH conditions. Alternatively, pH levels will tend towards neutral to slightly acidic with atmospheric CO<sub>2</sub>, subject to CO<sub>2</sub> partial pressures and Henry's law. With time and degradation of the concrete liner, the pH of dripping water will decline to neutral.

Under neutral (pH 4 to 9) or acidic conditions (pH<4), the corrosion of the carbon steel outer barrier will occur by cratering and uniform corrosion. Corrosion will begin with hemispherically shaped craters. Differences in O<sub>2</sub> transport will lead to greater attack of the non-cratered surface, and limitations in O<sub>2</sub> transport within the crater beneath the corrosion products will lead to lesser attack. Therefore, with time the craters will coalesce, and the surface will tend to level. Subsequent corrosion will occur as general corrosion, and a general corrosion rate can be used to describe this process.

---

<sup>3</sup> The justification for 120° is based on the assumption of the development of surface roughness due to corrosion and spalling, which allows dripping water to pool at sites despite a curvature approaching vertical.

### Pit Density Under High pH Conditions

Under elevated pH conditions ( $9 < \text{pH} < 13$ ), it is possible to passivate iron and also to develop high-aspect-ratio pits and crevices in carbon steel (Pourbaix, 1974). I expect that the locations where spalling of the oxide layer has occurred would have a slightly enhanced probability of localized pitting of the carbon. The spatial density of growing pits, given alkaline conditions, will decrease as a function of time. This is due to stifling of pits and the limited cathode area that supports the enlarging anode area as a pit grows. Figure JS-1 shows schematically the spatial density of pits {y-axis} in each range of pit depth {x-axis} as a function of time ( $t_1$ ,  $t_2$ , and  $t_3$ ). The right-hand peak should get smaller with time as pits stifle and as fewer pits continue to grow. The large left-hand peak remains at the same height, because these pits have already stifled. They may be metastable pits. Beginning at time  $t_1$ , the spatial density of growing pits is highest. At time  $t_2$ , the number of shallow pits is the same, but many growing pits in the right-hand peak stifle and the fewer remaining stable pits continue to grow toward the wall thickness. Likewise, at time  $t_3$  the number of growing pits is less still, but their depths have increased. A similar shape for pit distributions has been seen (Aziz, 1956). This relationship reflects the expected change in the number of growing pits as a function of time (or pit depth). Note that it is assumed that  $t_1$ ,  $t_2$ , and  $t_3$  occur after all initiation sites have been activated (i.e., there are no more initiation events). Thus, it is assumed that all pits initiate at  $t_{\text{early}}$  such that  $t_{\text{early}} \ll t_1$ .

This relationship reflects the expected change in growing pits as a function of time (or pit depth). Note that it is assumed that  $t_1$ ,  $t_2$ , and  $t_3$  occur after all initiation sites have been activated. Thus, it is assumed that all pits initiate at  $t_{\text{early}}$  such that  $t_{\text{early}} \ll t_1$ .

For carbon steel under alkaline conditions, I estimate that the initial (i.e.,  $t_1$ ) growing pit density (right-hand peak) will be the following (expressed as a cumulative distribution function, CDF). At early times, depth = 10 to  $10^4 \mu\text{m}$  (or  $10^{-3}$  to 1 cm).

Percentile of CDF

Growing Pit Density (pits/cm<sup>2</sup>)

99.9%

10

90%	1-2
50%	0.5
5%	??

I am saying that there is a 99.9% probability that there will be a maximum of 10 growing pits/cm<sup>2</sup> or less.

At later times, depths = 1 to 10 cm:

<u>Percentile of CDF</u>	<u>Growing Pit Density (pits/cm<sup>2</sup>)</u>
99.9%	2
90%	0.1-0.2
50%	0.01-0.02
5%	??

I am saying that there is a 99.9% probability that there will be a maximum of 2 growing pits/cm<sup>2</sup> or less in the depth range of 1 to 10 cm.

Quantifying the growing pit density into a finer pit depth scale soon after initiation.

Pit Depth = 1 to 10 μm

<u>Percentile of CDF</u>	<u>Growing Pit Density (pits/cm<sup>2</sup>)</u>
99%	1000
90	100
50	10
5	1

Addressing the issue of where these growing pit densities should be applied in modeling waste package degradation, the growing pit density depends on the amount of spalling of the oxide layer, and the chemistry, temperature, and ratio of halide ion concentration to that of the sum of the other anions. Recall that these densities apply only to the case of elevated pH, under dripping conditions, on the top of the waste package where bulk water exists.

In general it is true that lower pit densities and longer times to pit initiation have been observed when a thick magnetite film is formed. Two problems exist. First, the protection of

the prior thermal oxide against aqueous pitting has been observed only in short laboratory tests. A brief search revealed no long-term data. Secondly, there are reversals in the trend in that thick porous oxides sometimes produce greater pit densities/pit susceptibilities. Moreover, even in cases where the thermal oxide is beneficial, the result is a reduction in pit spatial density by a factor of 2 to 3. Therefore, I do not believe that much "credit" can be taken toward lower pit densities because of a thick oxide that does not spall. Only slight credit could be taken for such a reduction; pitting would not be stopped entirely. The exact degree of benefit would depend on structure, thickness, composition, growth rate, and porosity of the thermal oxides.

Factors that could change these growing pit densities are microbiologically influenced corrosion (MIC) and radiolysis. MIC could enhance localized attack of the carbon steel (i.e., an increased probability of initiation of new pits). As discussed later, radiolysis is not expected to be a concern in waste package degradation.

The diameter of growing pits in the carbon steel is estimated to range from 0.2 to 10 mm.

<u>Percentile of CDF</u>	<u>Pit Mouth Area</u>	<u>Pit Diameter</u>
99.9%	0.03 mm <sup>2</sup> to .79 cm <sup>2</sup>	0.2 to 10 mm
90	0.28 mm <sup>2</sup> to 0.246 cm <sup>2</sup>	0.6 to 5.6 mm
50	0.5 mm <sup>2</sup> to 2.27 mm <sup>2</sup>	0.8 to 1.7 mm

The assumption made here is that the pit mouth area is circular and has a radius equal to the pit diameter ÷ 2. This geometry is consistent with hemispherical and cylindrical pits.

This CDF says that I am 99.9% certain that growing pits are between 0.2 and 10 mm in diameter, etc.

The shape of a pit depends on a number of factors (Engelhardt and Strehblow, 1994). Pits grown at high potential under diffusion control often are hemispherical because the current

density is uniform at all positions on the pit surface. Crystallographic pits grown under charge-transfer control or ohmic control are more likely to achieve different current densities at different positions on the pit surface and therefore develop nonhemispherical shapes. I cannot estimate aspect ratios without specific information. Pits could transition from hemispherical to cylindrical or be dish-shaped (shallower than hemispherical), depending on conditions. One observation is that a few growing pits often transition to a cylindrical shape that has a high aspect ratio.

### **CORROSION RATES OF CARBON STEEL**

The corrosion rates for the carbon steel CAM vary as a function of the corrosion mode. Under neutral pH conditions, a general corrosion front will attack the CAM. Under high pH conditions, high-aspect-ratio pits will develop, and corrosion will occur due to the advancement of these pits as well as by slower general corrosion. Note that the passive current density on steel is a strong function of pH and temperature (M. Pourbaix, 1974). The passive current density on iron produces penetration rates much greater than 500  $\mu\text{m}/\text{yr}$  at a pH of 9 at room temperature. This finding cannot be neglected for a waste package even if pitting occurs at a faster rate.

In the case of neutral pH, the general corrosion rates that describe the rate of attack of the carbon steel as a function of time are the following. The general corrosion rate used in TSPA-95 for carbon steel seems reasonable. Because the corrosion of carbon steel under neutral conditions does not entail the development of true "pits" but, rather, a uniform general corrosion front with some roughness that should level with time, I do not recommend the use of a "pitting factor."

To describe the corrosion rate under high pH conditions, I recommend the use of a pit growth law rather than a pitting factor (which relates the growth rate of pits to the general corrosion rate). The pit growth law has the following form:

$$d = At + Bt_e^{n+1}$$

where  $d$  is the penetration depth,  $t_e$  is the elapsed time (time from initiation to a specified time), and  $B$  and  $n$  are constants.  $B$  and  $n$  are functions of the applied potential  $E_{app}$ , temperature,  $[Cl^-/SO_4^{2-}]$ , welding, aging time (e.g., metallurgical factors), and thickness of oxide film. Note that  $At$  accounts for general corrosion of the steel at the passive current density, which will occur much more slowly than localized pitting but will be a strong function of solution pH. It is assumed to produce linear penetration.

I define the value of  $n$  and its uncertainty by the following cumulative distribution function.

<u>Percentile of CDF</u>	<u>n-Value</u>
99.9%	-1.0 to 0.0
90%	-0.66 to -0.25
50%	-0.5 to -0.33

I am saying with 99.9% certainty that  $n$  is between -1 and 0. These results are based on the literature for iron and steel (Engell and Stolica, 1959; Tousek, 1972; Marsh et al., 1988; see Z. Szklarska-Smialowska, Pitting Corrosion of Metals, 1986 for additional references).

The depth  $d$  is equal to  $B$  when  $t_e = 1$  day. The following expresses my estimate and uncertainty in the value of  $d = B$  at  $t_e = 1$  day.

<u>Percentile of CDF</u>	<u>B (<math>\mu\text{m}/\text{day}^{n+1}</math>)</u>
99.9%	10,000
90%	1,000
60%	800
40%	200
10%	100
0.1%	10

I am saying that there is a 99.9% probability that B is 10,000 or less, etc.

This is based my experience: I have never seen pits larger than 1 cm in depth after one day, even during very aggressive exposure conditions. One is more likely to find a pit of several hundred microns or less after one day. My experience also tells me that it is difficult for a growing pit to remain active if the pit depth is less than 10 micrometers after 1 day. Experimental work could be conducted to reduce this large range of uncertainty.

In addition to pit stifling, the value of  $n + 1$  might decrease over long periods as growing pits compete for limited cathode area. For example,  $n + 1$  might decrease from 0.5 to 0.25 over long periods. This often is reflected in exposure data, which show that pit depths usually are less than in the case of potentiostatic polarization (Marsh et al., 1988). In laboratory tests using potentiostats, cathode-limited pit growth does not occur, and constant applied potentials can be maintained. This differs from actual exposure situations.

### **ALTERNATIVE CORROSION-ALLOWANCE MATERIAL**

Monel alloy 400 should exhibit significantly slower dry air oxidation kinetics than steel, should experience lower rates of humid-air corrosion, and should undergo uniform aqueous corrosion in slightly acidic, neutral, or slightly alkaline pH more slowly than steel because of the lower passive dissolution kinetics of nickel compared to iron at the same pH and temperature. Passive dissolution should occur in a pH range equivalent to and likely broader than that for iron. It should not be difficult to obtain some information on penetration or oxide growth rate for the corrosion of 70%Ni-30%Cu alloy in each of these environments. This information could be used to test the impact of the lower corrosion rates on this Ni-base material for the TSPA. The suppression of pH due to hydrolytic acidification would be minimal for this Ni-Cu alloy because of the weak hydrolysis of Ni and Cu cations compared to the strong hydrolysis of  $\text{Fe}^{+2}$  and  $\text{Fe}^{+3}$  and the lower dissolution rates for Monel 400<sup>4</sup>. An

---

<sup>4</sup> Note that the pH for the hydrolysis reaction  $\text{Ni}^{+2}/\text{Ni}(\text{OH})_2$  is given by  $\text{pH} = 6.09 - 0.5 \log[\text{Ni}^{+2}]$  which is similar to  $\text{Fe}^{+2}/\text{Fe}(\text{OH})_2$ ;  $\text{pH} = 6.64 - 0.5 \log[\text{Fe}^{+2}]$ . However, the  $\text{Fe}^{+2}/\text{FeOH}^+$

interesting question for pH suppression of the steel CAM is whether  $\text{Fe}^{+2}$  will slowly become oxidized to  $\text{Fe}^{+3}$  in the crevice region between the CRM and CAM. The presence of non-polarizable Fe and  $\text{Fe}_3\text{O}_4$ , as well as oxygen depletion in crevices, makes  $\text{Fe}^{+3}$  production unlikely except in severely corroded regions away from the steel. Monel 400 suffers localized corrosion via concentration of metal ions instead of by dissolution/hydrolysis/acidification. However, Monel 400 has other corrosion vulnerabilities that produce more insidious corrosion modes (e.g., dealloying; activation in the presence of sulfide, such as in  $\text{H}_2\text{S}$ ; in the presence of MIC). The modeling of the dealloying process would be more complex than a 4x increase in corrosion rate that could be applied to the MIC of steel. However, I do not believe that there is a reported instance of catastrophic failure of Monel 400 due to dealloying. Localized corrosion can occur (Gdowski, 1991) in the form of pitting and crevice corrosion, but this occurs by the metal ion concentration cell mechanism (as highlighted in the original report for Table 31, this occurs outside and adjacent to crevice formers). Monel 400 is resistant to stress corrosion cracking (SCC) and hydrogen embrittlement. Long-term exposure at elevated temperatures has been noted to produced some intergranular cracking in wet steam lines in Naval applications (Private communication, Tom Montemarano, NSWC-Carderock). In summary, this material performs poorly compared to a corrosion-resistant alloy such as alloy 825 or 625 (Gdowski, 1991, Table 31), but the real opportunity/benefit has to do with whether it significantly improves dry oxidation, humid-air, and aqueous corrosion rates as a CAM material compared to steel. Significant improvement in this category is likely. There may be some concern that the copper content could be detrimental to the CRM in the inner liner (Stahl, WPDEE Workshop 2-3). Alloyed Cu content degrades the localized corrosion behavior of Fe-base Incolloys, but not Ni-Cr-Mo-F alloys such as 625 or C-22 (private communication with Ed Hibner, Huntington Alloys International, July 1997). Moreover, galvanic coupling between alloy 625 and Monel in seawater caused galvanic corrosion of the Monel but did not affect the 625. In fact, slight galvanic suppression of C-22 or 625 localized corrosion might be achieved,

---

hydrolysis reaction gives  $\text{pH} = 4.75 - 0.5 \log [\text{Fe}^{+2}]$ .  $\text{Fe}^{+3}$  hydrolysis can decrease the pH to 1.5. Ref: M.H. Peterson, T.J. Lennox, R.E. Groover, Mater. Prot., p. 23, 1970.

because Monel 400 does not develop biofilms as readily in seawater. Thus potential ennoblement by biofilms is suppressed (Scully and Hack, 1986; Scully et al., 1986).

### **CORROSION OF CORROSION-RESISTANT INNER BARRIER**

The degree to which the CAM will protect the CRM through galvanic suppression is a direct function of the nature of the assumed thin electrolyte film or Fe-base corrosion products that are expected to form in the corroded regions of the CAM and the aspect ratio of "pits" or the morphology of the general corrosion front of CAM that develops. Given the expected thin film/corrosion products that are expected for the given bulk water conditions, the throwing power is expected to be small (distances on the order of millimeters or, at most, centimeters).

The benefit would be to reduce galvanic couple potentials below threshold potentials for crevice, pitting, and perhaps stress corrosion. For instance, the crevice propagation potential for 625 in 0.6 M NaCl was near 0  $V_{scc}$ . Crevice propagation was halted below this potential (Lillard et al., 1994).

Figure JS-2 illustrates schematically the process of galvanic coupling between the CAM and the CRM. Assuming neutral pH conditions, the morphology of the general corrosion front will be a rough surface lacking high-aspect-ratio pits. As a result, once penetration of the CAM begins, the CRM will become exposed rapidly over large surfaces. At the first penetrations, the CRM will be galvanically protected. With continued advancement of the corrosion front and widening of the exposed CRM area, crevices likely will form beneath the CAM. These shrink-fit crevices likely would fill with solution because of capillary action. These crevices will be galvanically protected but, because of short throwing distances, the central exposed CRM area will not. With continued corrosion of the CAM and oxidizing conditions,  $Fe^{+2}$  in solution will be oxidized to  $Fe^{+3}$  at some positions and will temporarily raise the mixed potential. However,  $Fe^{+2}$  is expected in regions in contact or within close proximity to the remaining non-polarizable steel. When all steel has dissolved, oxidized iron will exist as  $Fe^{+3}$  and  $Fe_2O_3$ , depending on pH and temperature. Alloys 625 and C-276 would experience localized corrosion vulnerability in  $FeCl_3$  at elevated temperature. Based on this scenario for the corrosion of the CAM under neutral conditions, I would not expect a

long period of galvanic protection of the CRM—well less than 1000 years. For instance, if the CAM thickness at the least-corroded spots was 1 cm (see Figure JS-1), and the galvanic corrosion rate of steel remained a modest 5 to 10 mils/yr (125 to 250  $\mu\text{m}/\text{yr}$ ), then the remaining CAM steel would be corroded away in 40 to 80 years. However, near the end of this process the galvanic corrosion ratio would increase as the cathode area increased; a constant dissolution rate was assumed here instead of a constantly changing anode/cathode area ratio that accelerates the galvanic corrosion rate. In the case of perfectly uniform general corrosion of the CAM (JS-2 bottom figure), no galvanic interaction occurs because the CAM is uniformly thinned.

Assuming high pH conditions and the expected development of high-aspect-ratio pits in CAM, galvanic suppression is expected to be operative. However, as pH conditions in the potential repository return to neutral (following degradation of the concrete liner), general corrosion processes will prevail, and the high-aspect-ratio pits will be overcome by the general corrosion front. Assume, for example, passive dissolution of the steel to a 5 to 7-cm thickness and a few surviving 5 to 7-cm-deep penetrating pits that are spaced 5 to 10 cm apart growing to reach the CRM to enable a galvanic interaction. In this case, galvanic corrosion at 5 to 10 mpy (125 to 250  $\mu\text{m}/\text{yr}$ ) could occur for 200 to 400 years before the period of galvanic suppression would end. Initially, the area ratio would be more favorable to the steel anode, because small areas of CRM cathode would be exposed. Note that the actual galvanic corrosion rates could be greater.

### **Pit Initiation**

It first is assumed that pits initiate only in regions where there is bulk water from dripping. It is minimal under humid-air conditions that do not produce bulk water by capillary condensation. The probability of pit initiation depends critically on the electrochemical potential achieved by the CRM, temperature, salinity,  $C_{r_{equiv}}$ , solution pH, etc. For instance, a metastable pit initiation function might have the following dependencies:

$$\lambda \text{ (metastable pits/cm}^2\text{-sec)} = \lambda_0 \exp (-Bt)$$

where  $\lambda_o$ , B = function of  $E_{app}$ , temperature,  $[Cl/SO_4^{2-}]$ ,  $Cr_{eq}$  of Ni-Cr-Mo superalloy, welding, aging time (e.g., metallurgical factors), and thickness of oxide film; t is elapsed time under a given set of conditions.

$$\lambda_o = \text{constant} * \log [Cl/SO_4^{2-}] * \exp[E_{app}] * \exp(-Q/RT) * [Cr_{eq}]^n$$

Here Q is an activation energy. It is interesting to note that 24-hour exposure at 70°C in 3.8% FeCl<sub>3</sub> produced localized corrosion on 825 above -100 mV<sub>SCE</sub>, above +400 mV<sub>SCE</sub> for alloy 625, and above 800 mV<sub>sce</sub> for C-276 (Asphahani, 1980). This supports the trends shown on Figure JS-3 if all data are shifted 300 mV to the right for pitting. The current trends on Figure JS-3 might better represent localized crevice corrosion trends.

Clearly, MIC biofilms, H<sub>2</sub>O<sub>2</sub>, and Fe<sup>+3</sup> raise the applied potentials shown on Figure JS-3. Intrinsic material susceptibility for steel, 625, C-276, and C-22 are shown schematically. Note that the data are highly schematic; experimental data are required. The justification for the distribution is based on data by Shibata, for instance, for a lab-sized specimen (Shibata and Takeyama, 1977; Shibata and Takamiya, 1986; Henshall, 1992; Mola et al., 1990; Williams et al., 1985a, 1985b; Reigada et al., 1994; Wu et al., 1997; Lunt et al., 1997).

For a lab-sized at-risk surface area (cm<sup>2</sup>), there is a finite probability of having a fatal flaw that initiates a pit or crevice corrosion. Therefore, if a waste package is divided into regions approximately cm<sup>2</sup>, the probability of initiation at each site as a function of its electrochemical potential can be defined for the conditions shown. The dotted lines for each alloy indicate qualitatively how the probability of initiation is shifted to higher or lower potential depending on whether temperature is lower or higher and the ratio of Cl/anions represented by  $[Cl/SO_4^{2-}]$  is lower or higher. For instance, pitting potentials decrease about 100 mV for an order-of-magnitude increase in  $[Cl/SO_4^{2-}]$ . Pitting potentials decrease about 4 mV per °C increase in temperature above 25°C (A. Roy, WPDEE Workshop 1; Semino et

al., 1979). A given alloy might have slightly lower or higher  $Cr_{equiv}$  if weld dilution occurs, where one definition of Cr equivalency is:

$$Cr_{eq} = Cr + 1.6 Mo + 4.3 Nb + 7W \text{ (wt.\%)}$$

(ref: E. Hibner, CORROSION/86, Paper 181)

Overlap of electrochemical potentials experienced by the CRM having the material behavior indicated by solid or dotted lines provides information on the probability of pit initiation and pit density.

### Penetration Rates

The expected corrosion mode of the CRM is development of high-aspect-ratio pits and crevice corrosion. Therefore, the assessment of pit/crevice growth rates is similar to that for the corrosion rate of the CAM under high pH conditions, except that higher potentials, temperatures, and salinity levels are necessary to enable such localized corrosion processes. However, an assessment must be made of the probability of initiation of stable pits or, equivalently, the initial density of growing pits. As shown schematically on Figure JS-3, the probability of pit initiation is a function of the applied potential  $E_{app}$ , temperature,  $[Cl-/SO_4^{2+}]$ , pH, and  $Cr_{equiv}$ . Increasing temperature,  $E_{app}$ , and  $[Cl-/SO_4^{2+}]$ , and decreasing  $Cr_{equiv}$  and pH create more aggressive conditions; the density of growing pits increases as the former three factors increase.  $Cr_{eq}$  is reflected in the CRM material in that a lower  $Cr_{eq}$  produces a greater density of pits at any given temperature,  $E_{app}$ , and  $[Cl-/SO_4^{2+}]$ .

The same relationships can be used for the initial density of growing pits except that the range of 10 to 0.1 pits/cm<sup>2</sup> might be tighter. The potential range shown was hypothesized based on the distributions in observed pitting potentials. The range of growing pit densities is shown as CDFs for given conditions and alloys. The position of these CDFs is unknown because of insufficient data and must be established experimentally. Therefore, the numbers on the axes are to be taken as completely hypothetical. The far left curve is for steel,

followed by 625, C-276, and C-22. Experiments are needed to establish the probability of pit initiation (or initial growing pit densities) as a function of applied potential for given temperatures and alloys, particularly focusing on C-22, for which few experimental data exist. Also shown on the figure are the possible mixed potentials established for a complete MIC biofilm (~200 to 300mV) and for  $\text{Fe}^{+3}/\text{Fe}^{+2}$  (~400mV, for equal concentrations of  $\text{Fe}^{+3}/\text{Fe}^{+2}$ ; the redox potential for this reaction is +530 mV<sub>sce</sub>, but the equilibrium potential is  $E = 530 \text{ mVsce} + 59 \text{ mV} \log(\text{Fe}^{+3}/\text{Fe}^{+2})$ ).

Given pit initiation, the expected change in density of growing pits with time is expected to follow the relationship discussed for the CAM in the high-pH case. Likewise, the pit growth law will have the same form:

$$d = Bt_c^{n+1}$$

The values of B will be similar for the CAM, but the values of n will differ as a function of the alloy assumed for the CRM. Stable growth does not occur unless the CRM experiences more positive potentials. Again, the assessment of n-values as a function of applied potential  $E_{\text{app}}$  should come from experimental data measured at various temperatures and  $[\text{Cl}^-/\text{SO}_4^{2-}]$ . Figure JS-4 shows a hypothetical relationship between  $E_{\text{app}}$  and n+1. The n-values are expected to fall within the range of -0.75 to -0.25, with the same uncertainty as expressed for the steel. This assertion is based on literature results for stainless steels and Ni; results should be obtained for the alloys of interest (Garz et al, 1969; Forchhammer et al, 1969; Szklarska-Smialowska, 1971; Rozenfeld and Danilov, 1970; Hunkeler and Boehni, 1984; Alkire et al., 1998 [?]; Hunkeler and Boehni, 1987).

It should be recognized that n+1 values might become truncated at 0.5 (n = -0.5) with applied potential if diffusion-limited pit growth occurred. That is to say that n + 1 would not continue to increase with potential, etc. Changes in B with acceleration variables (potential, temperature, etc.) might also be considered. In addition to pit stifling (to be discussed below), the value of n + 1 might decrease over long periods as growing pits compete for limited cathode area as discussed above for steel. Recall the plot of penetration depth as a

function of time presented by D. Shoemith at WPDEE Workshop 3. For example,  $n + 1$  might decrease from 0.5 to 0.25 over long periods. This is often reflected in exposure data, which show that where pit depths are usually less than in the case of potentiostatic polarization (Marsh ref). In laboratory tests using potentiostats, cathode-limited pit growth does not occur, and constant applied potentials can be maintained. This differs from actual exposure situations. Therefore, the effect of time on  $n + 1$  should be considered.

Of course, more aggressive threshold conditions are required for pit initiation on more noble metals; however, once initiated, the rates of pit penetration would follow a similar form of growth law.

#### **Pit/Crevice Stifling**

A rational technical basis for stifling of pits and crevices is needed before pit stifling should be assumed. There are several technical reasons for stifling.

1. Cathode-limited pit/crevice growth. Probability of this is high in thin film electrolyte.
2. Preferential dissolution and beneficial enrichment of alloying elements that lower dissolution rates in pits/crevices until repassivation occurs.
3. Growth of the pit/crevice into a more open geometry that no longer favors concentration of a depassivating pit/crevice solution and/or provides enabling ohmic potential drop.
4. Growth laws that do not favor maintenance of the concentrated pit electrolyte.

The probabilities of all these phenomena are unexplored for the alloys and environments proposed. For instance, with regard to stifling mechanisms 1 and 4, it is reasonable to hypothesize that if pit growth rates become too slow (for example due to cathodic limitations), then the pit environment might become diluted. Consider pit growth. When  $E_{app}$

>  $E_{\text{repass}}$ , the probability of pit death becomes low, or the transition to stable pit occurs and a pit growth law might be defined as:

$$i_{\text{pit}} = Ct^n$$

$$d_{\text{pit}} = Bt_c^{n+1}$$

where  $i_{\text{pit}}$  is the pit current density;  $t$  is time; and  $C$ ,  $B$ , and  $n$  are constants. Assume a cylindrical pit having a constant area at its bottom.  $C$ ,  $D$ , and  $n$  are functions of  $E_{\text{app}}$ , temperature,  $[\text{Cl}/\text{SO}_4^{2-}]$ ,  $\text{Cr}_{\text{eq}}$  of Ni-Cr-Mo superalloy, welding, and aging time (e.g., metallurgical factors). Recall that pit stabilization occurs when:

$$i_{\text{pit}} \times \text{depth}_{\text{pit}} \geq \text{critical value}$$

because the critical value is fundamentally related to the concentration of the depassivating pit chemistry. When  $n$  is  $-0.5$ , this chemistry is maintained with growth time for a cylinder geometry growing at its bottom. However, if  $n$  is more negative than  $-0.5$ , the pit/crevice may die/stifle as long as the mouth is not blocked against transport. For example if  $n = -0.66$ , a criterion for stifling emerges:

$$\text{Pit solution concentration} \approx i_{\text{pit}} \times \text{depth}_{\text{pit}} = C \cdot D \cdot t^{2n+1} = C \cdot D \cdot t^{-0.33}$$

Notice that in this case the solution concentration in the pit is decreasing with growth time. Eventually the pit repassivates. I speculate that some of the slow rates of pit growth reported under natural exposure conditions actually are a reflection of pit death.

### Passive Dissolution Rate of CRMs

The passive dissolution rates of the CRMs will depend strongly on temperature, pH, and time and weakly on potential and  $[\text{Cl}/\text{SO}_4^{2-}]$ . The passive dissolution rates will be highest at high temperature and low pH, but under all conditions should decrease with time by orders of magnitude. Initially, under the most aggressive conditions the rate could be as high as 500

$\mu\text{m}/\text{yr}$ , but even under these conditions could decrease with time to 5 to 50  $\mu\text{m}/\text{yr}$  as oxide films thicken. The passive dissolution rate under neutral or alkaline conditions at temperatures approaching room temperature could start at 5 to 50  $\mu\text{m}/\text{yr}$  and decrease to as low as 0.05 to 0.005  $\mu\text{m}/\text{yr}$  with time. Declining temperatures of the waste package surfaces should serve to further lower passive dissolution rates. This is based on laboratory polarization curves and potential holds near room temperatures. However, data from alloy manufacturers that find passive dissolution rates on these alloys of  $< 50 \mu\text{m}/\text{yr}$  in aggressive, near-boiling solutions is disconcerting in that these rates, if sustained, could be troublesome over long periods. Again, the same issue applies as to low-temperature CAM oxidation rates. Long-term data are limited: the rates of the applicable corrosion processes may be slow or negligible for 20-year structural lifetimes, but worth consideration for 1000s of years.

### **MICROBIOLOGICALLY INFLUENCED CORROSION**

MIC potentially will occur after repository conditions have cooled below about 100°C and relative humidity is above about 60 percent. The maximum area that might be affected by MIC is the area of the waste package that is subjected to dripping conditions, required to provide a sufficient water supply for microbial growth. The actual area affected probably will be less. If the drips are intermittent, MIC will occur during the dripping periods, stop during the dry periods, and restart with additional drips. The effect on the CAM will be to lower the pH to 4. I suggest that MIC will result in a 2x to 5x multiplier on the corrosion rate for the CAM. The effect on the CRM would be to increase the open-circuit potential to about 200 to 300 mV and thus enhance the probability of pit/crevice initiation on alloy 625, for instance, but not on C-22 (Kain, 1993; Dexter et al., 1994, 1989, 1990, 1996).

The increases in potential to +200 to 300 mV<sub>sc</sub> might be limited with respect to surface area, because a MIC film that covers completely might not be possible. The effects of MIC on Monel 400 would be different in that other corrosion vulnerabilities might come into play (e.g., dealloying).

---

## OTHER ISSUES

### Radiolysis

High pH conditions that occur as a result of drips through the concrete after temperatures have declined to below the boiling point (discounting the minor elevation of boiling point due to electrolytes) are not expected to occur until about 1000 years after emplacement of the waste packages. At a half-life of 30 years for Cs-137 (one of the major radionuclides contributing to radiation dose), the radiation dose will be too small at that time to cause significant radiolysis effects.

### Welds

A simple way to abstract the behavior of CRM welds relative to the base alloy would be to consider it in terms of  $Cr_{equiv}$ . Lower  $Cr_{equiv}$  would result in enhanced susceptibility to localized corrosion as detailed in my WPDEE Workshop 3 presentation. This would be the primary factor affecting initiation and growth if weld dilution of base compositions occurred. A secondary factor would be the effect of a heat tint on resistance to localized corrosion. A porous heat tint oxide often lowers corrosion resistance.

### Ceramic Coating

Ceramic coatings should delay the spread of corrosion processes on the CAM outer liner and CRM inner liner until significant fractions of the ceramic are spalled. However, because all coatings will contain some defects (cracks or flaws) from placing the canisters, I expect that the time to first penetration would not be reduced significantly. This is because at such defects the exposed steel experiences dry oxidation, humid-air corrosion, aqueous corrosion, and galvanic coupling to the CRM as without any ceramic coating. The mode of corrosion of the CAM is not expected to differ from the case of no ceramic coating. The aqueous solution in cracks might become acidic from ferrous and ferric ion hydrolysis, enabling acidic uniform corrosion of the steel outer coating barrier. However,  $O_2$  transport rates likely would be slower through pores and cracks in a ceramic coating. More voluminous corrosion products (Billing-Bedworth ratio) then would serve to spall the low-fracture toughness ceramic from these positions. Moreover, cracks in the ceramic coating might serve as positions for early

---

capillary condensation, promoting the presence of bulk water at a slightly earlier point in the humid-air exposure stage. The critical calculation would be how much credit (what period of time) can be granted for a reduced area of exposed CAM, and subsequently exposed CRM, before ceramic coating spalling removes a significant fraction of the ceramic coating. One could envision taking "credit" for the ceramic over a decreasing percentage of the waste package surface area. Once spalling initiates, it is likely to proceed rapidly. The net effect is a delay in corrosion processes over a decreasing percentage of the waste package surface area.

## REFERENCES

- Alkire, R.C., and Wong, K.P., 1998, *Corros. Science*, 28(4), p. 411-421. [1998?]
- Asphahani, A.J., 1980, *Materials Performance*, 19(8), p. 9.
- Aziz, P.M., 1956, *Corrosion*, 12, p. 35.
- Davies, D.E., Evans, U.R., Agar, J.N., 1954, *Proc. Royal Soc.*, A225, p. 443.
- Davies, M.H., et al., 1951, *Journal of Metals NY*, 3, 889.
- S.C. Dexter, et al., 1996, *Effect of Biofilms on Crevice Corrosion, Proceedings of the Corrosion/96 Research Topical Symposia -Part II: Crevice Corrosion: The Science and its Control in Engineering Practice*, p. 367.
- S.C. Dexter, et al., 1994, *Biofouling Effects on Corrosion of Stainless Alloys in Seawater, Biodeterioration Research* 4, p. 533.
- S.C. Dexter, et al., 1990, *Effect of Biofilms on Corrosion Potential of Stainless Steel Alloys in Estuarine Waters, 11th International Corrosion Congress, Florence, Italy, Vol. 4*, p. 4.333.
- S.C. Dexter, et al., 1989, *Effect of Biofilms on Crevice Corrosion of Stainless Steels in Coastal Seawater, Corrosion J.*, 51(1), p. 56, 1995. also see Discussion of same in *Corrosion J.* 45(10), p. 786.
- Engelhardt, G., and Strehblow, H.H., 1994, *Corrosion Science*, 36, p. 1711-1725.

- Engell, H.J., and Stolica, N.D., 1959, Z. Phys. Chem., NF, 20, p. 113.
- Forchhammer, P., and Engell, H.J., 1969, Werkst. Korros., 21, p. 1.
- Garz, J., Worch, H., and Schatt, W., 1969, Corros. Science, 9, p. 71.
- Gdowski, 1991, Survey of Degradation Modes of Four Nickel-Chromium-Molybdenum Alloys, March Report, UCRL -ID-108330.
- Graham, M.J., Ali, A.I., Cohen, M., J., 1970, Electrochem. Soc., 117, p. 513.
- Gulbransen, E.A., and Roswell, R., 1950, Journal of Metals, N.Y., 188, p. 500.
- Henshall, G.A., 1992, J. Nuclear Materials, 195, p. 109.
- Hunkeler, F., and Boehni, H., 1987, In Advances in Localized Corrosion, NACE-9, p. 69.
- Hunkeler, F. and Boehni, H., 1984, Corros. J.
- Kain, R.M., 1993, Seawater Testing to Assess the Crevice Corrosion Resistance of Stainless Steels and Related Alloys, Paper No. 347, 12th International Corrosion Congress.
- Lillard, R.S., Jurinski, M.J., and Scully, J.R., 1994, Crevice Corrosion of Alloy 625 in Chlorinated ASTM Artificial Ocean Water, *Corrosion J.*, 50(4), p. 251-265.
- Lunt, T.T., Pride, S.T., Scully, J.R., Hudson, J.L., and Mikhailov, A.S., Cooperative Stochastic Behavior in Localized Corrosion, II. Experiments, J. Electrochem. Soc., 144(5), p 1620, 1997.
- Marsh, G.P., Bland, I.D., and Taylor, K.J., 1988, Br. Corros. J. 2393, p. 157.
- Mola, E.E., Mellein, B., Rodriguz de Schiapparelli, E.M., Vicente, J.L., Salvarezza, R.C., and Arvia, A.J., 1990, J. Electrochem. Soc., 137, p. 1384.
- Pourbaix, M., 1974, Atlas of Electrochemical Equilibria in Aqueous Solutions, Z. Szklarska-Smialowska Pitting Corrosion of Metals, p. 315. [Same as next?]
- Pourbaix, M., 1974, Atlas of Electrochemical Equilibria in Aqueous Solutions, NACE, p. 315.

Reigada, R., Sagués, F., and Costa, J.M., 1994, *J. Chem. Phys.*, 101, p. 2329.

Rozenfeld, I.L., Danilov, I.S., 1970, *Zashita Metallov*, 6, p. 14.

Scully, JR., and Hack, H.P., 1986, Galvanic Corrosion Prediction Using Long and Short Term Polarization Curves, *Corrosion J.*, 42(2), February.

Scully, JR., Hack, H.P., and Tipton, D.G., 1986, Effect of Exposure Time on the Polarization Behavior of Marine Alloys under Flowing and Quiescent Conditions, *Corrosion J.*, 42(8), August.

Semino, et al, 1979, *Corros., Sci.* Vol. 19.

Shibata, T., Takamiya, H., 1986, In Critical Issues in Reducing the Corrosion of Steels, NACE, p. 17.

Shibata, T., Takeyama T., 1977, *Corrosion J.*, 33, p. 243.

Szklarska-Smialowska, Z., 1971, *Werkst. Korros.* 22, p. 780.

Tousek, J., 1972, *Corrosion Science*, 12(1).

Williams, D.E., Westcott, C., and Fleischmann, M., 1985a, *J. Electrochem. Soc.*, 133, p. 1796.

Williams, D.E., Westcott, C., and Fleischmann, M., 1985b, *J. Electrochem. Soc.*, 133, p. 1804.

Wu, B., Scully, J.R., Hudson, J.L., and Mikhailov, A.S., 1997, Cooperative Stochastic Behavior in Localized Corrosion, I. Model, *J. Electrochem. Soc.*, 144(5), p 1614.

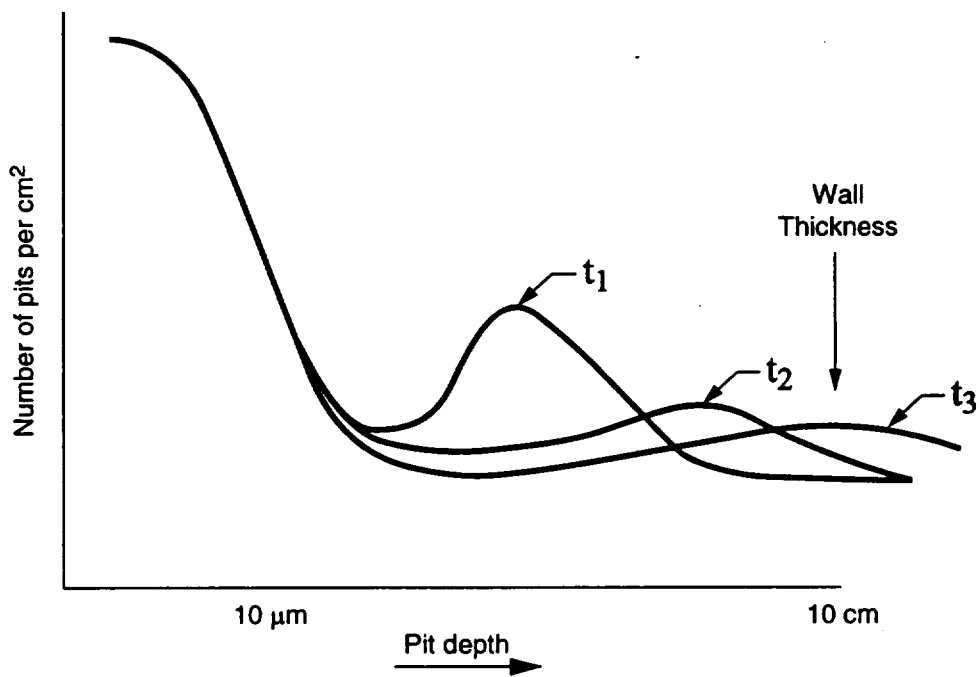


Figure JS-1 Schematic relationship between pit density and maximum pit depth as a function of time ( $t_1, t_2, t_3$ ). Assumes that all pits have initiated at  $t_1$ .

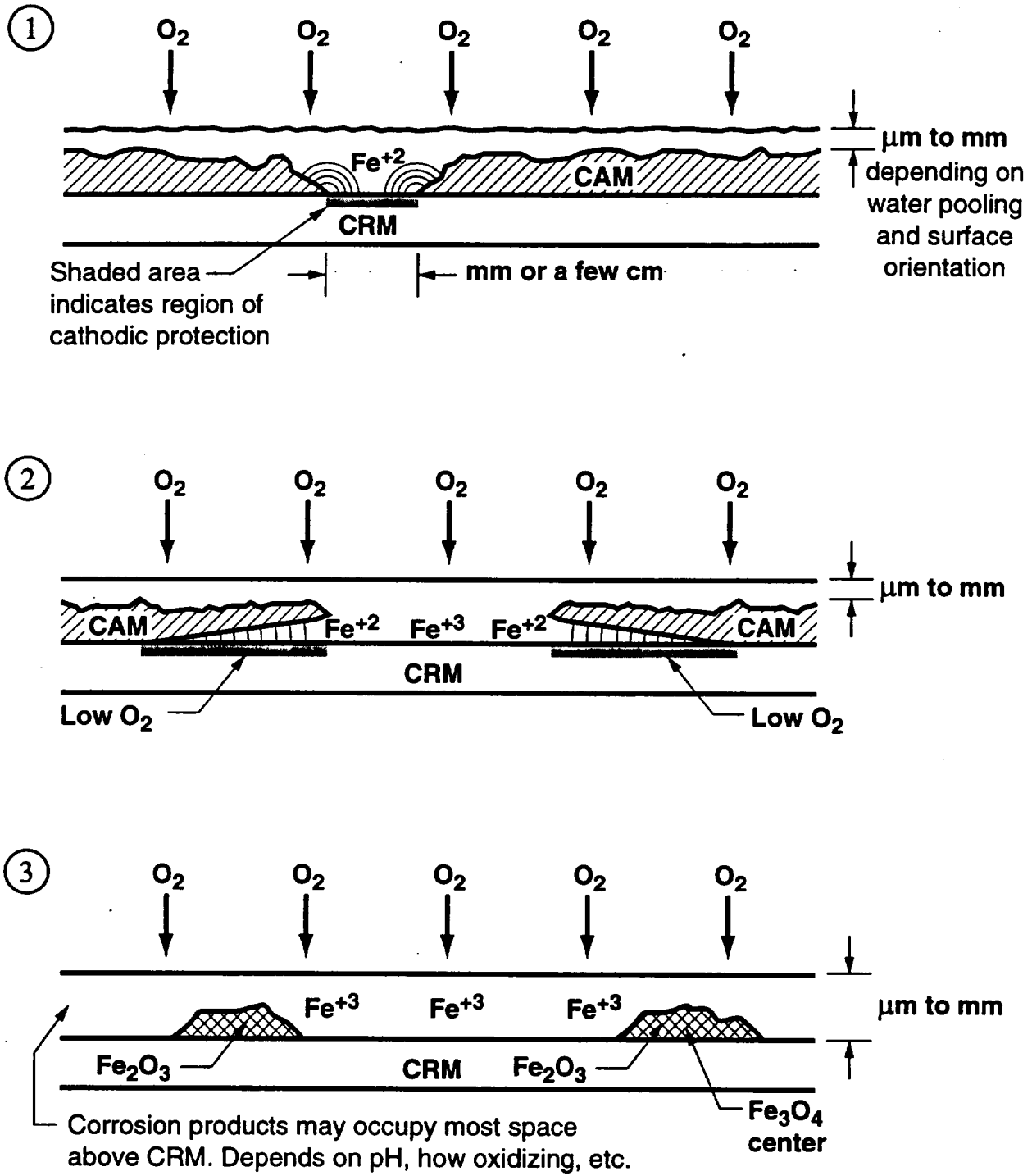


Figure JS-2 Galvanic coupling to steel

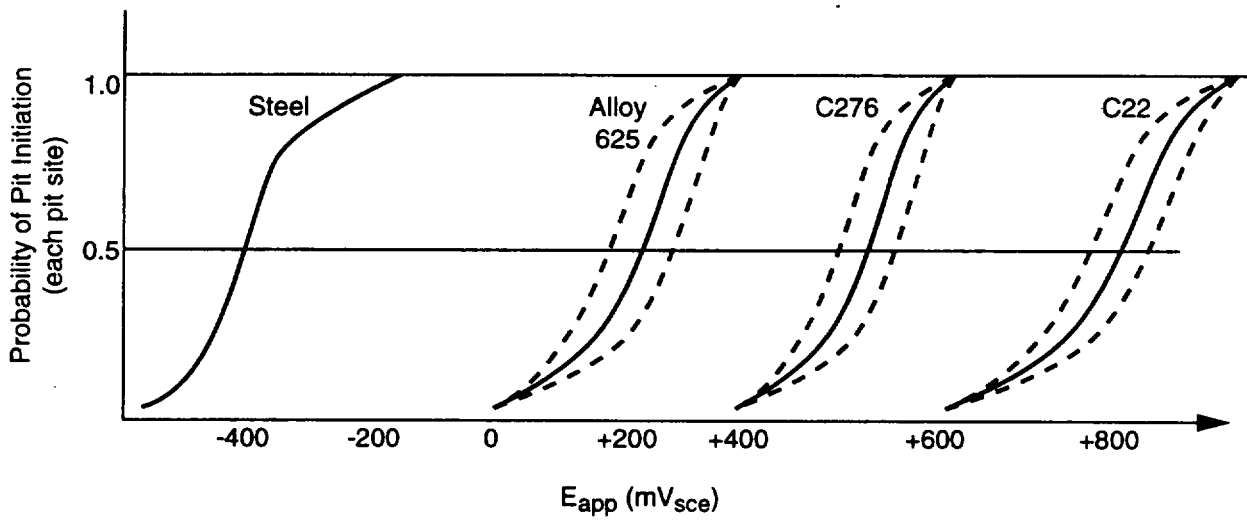
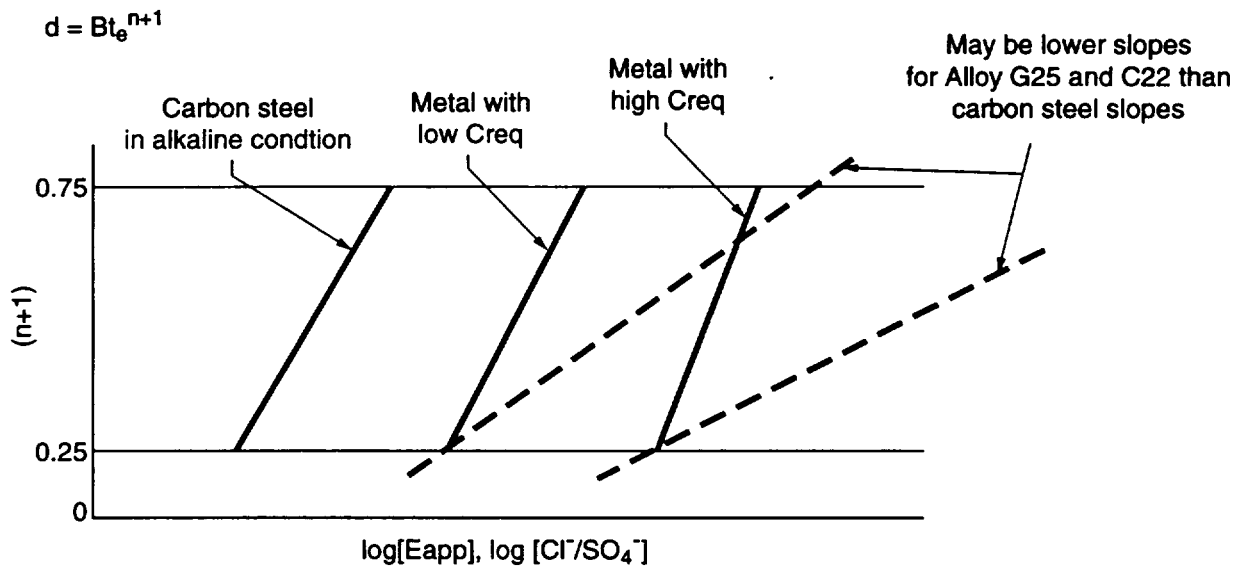


Figure JS-3 Hypothetical relationship between electrochemical potential and probability of pit initiation for CAM and CRM materials. Dotted lines to the left for each alloy indicate increased susceptibility with higher temperature, higher  $[Cl^-/SO_4^{2-}]$  ratio, etc. Dotted lines to the right indicate low temperature  $[Cl^-/SO_4^{2-}]$  ratio, etc.



Note: Higher potential (E) for pit initiation for more noble metals, but once initiated, the pitting n+1 growth factor would be about the same

Figure JS-4 CRM growth law

---

**ELICITATION SUMMARY**  
**DAVID W. SHOESMITH**

**OVERVIEW OF WASTE PACKAGE CORROSION PROCESSES**

The time-evolution of waste-package degradation processes is best viewed by considering the evolution of bulk environmental conditions over the life of the potential repository. Figure DS-1 shows schematically the general changes in key conditions with time, including the temperature, relative humidity (RH), oxygen availability, salinity of water contacting the package, pH of dripping water and water films, and precipitation and redissolution of deposits on the waste package. Of these conditions, the reference conditions to be assumed for the surface of the package were provided for temperature and relative humidity. It is assumed that during the early period of high temperatures and low RH, there will be no dripping water into the drifts. The first occurrence of dripping water will quickly evaporate, leaving salt deposits on the surface. With increasing moisture, the salinity of any water on the container surface will be relatively high, because of the salt deposits and the iron oxide developing on the surface of the container. This salinity will decrease gradually with time and increased relative humidity. With further cooling and the possible introduction of more drips, the water entering the drifts by percolation through the concrete lining likely will have elevated pH. With degradation of the concrete through time, the pH of the free water will decrease gradually to neutral. It is assumed that throughout the life of the repository, the availability of oxygen will be high. Although oxygen may be depleted during the hot period by boiling/sparging, this is unlikely to have a significant influence on the dry oxidation process that will prevail during this period.

With the time-evolution of environmental conditions will come an evolution of corrosion processes, as shown diagrammatically on Figure DS-2. During the early hot/dry period, corrosion will occur at a very slow rate through dry oxidation of the carbon steel corrosion-allowance material (CAM). A very thin (likely microns in thickness) oxide layer will

develop during this period. This oxide layer will not become thick because of high-field ion conduction. The film will grow by ionic transport through the thickening oxide. The rate of this process will be controlled by the field across the thickening film, which decreases rapidly with minor film growth. For even a relatively thin oxide film, the ionic transport rate becomes negligibly small quickly as the film effectively achieves a limiting thickness. This film will possess a lower density than the substrate metal and cannot grow without the buildup of stresses in the film. The need to relieve these stresses can lead to cracking of the oxide and spalling. For the warm conditions (200° to 140°C) prevailing at short times in the repository, the limiting film thickness is likely to be reached before the critical stress for cracking. Consequently, spalling of the oxide is unlikely. Temperatures of a few hundred degrees are needed for significant spalling to occur. Any spalling that does occur is expected to repair itself by the formation of another oxide layer. Irrespective of whether spalling actually does/does not occur, the data used in TSPA-95 to determine the time dependence for general corrosion in both humid air and aqueous solutions was recorded on specimens not subjected to a pre-period of dry oxidation. Therefore, a film which could possibly be subject to spalling was not present at the onset of corrosion. Consequently, the use of this data in assessment calculations ignores any possible protectiveness of the film formed during dry oxidation. Its use is, therefore, equivalent to assuming all the preformed oxide has spalled from the waste package surface.

The onset of any significant corrosion will begin when temperatures fall below about 100° to 120°C and relative humidities are greater than about 70 percent. With the onset of these conditions will come humid-air corrosion of the CAM through both general corrosion and pitting of the carbon steel. Once the humidity achieves a value at which humid corrosion can be sustained, the potential for microbiologically influenced corrosion (MIC) is present.

At lower temperatures and higher RH, including localized drips, aqueous corrosion processes will ensue. Eventually, the CAM will be penetrated and there will follow a period of galvanic protection of the corrosion-resistant material (CRM). Because of the morphology of the corrosion front in the CAM (discussed later), I do not expect this period of galvanic protection to last very long. The nature of the corrosion processes affecting the CRM will

depend on the material chosen. For a nickel alloy with a sufficiently high Mo/Cr content (e.g., C22), localized corrosion should not occur and general passive corrosion should proceed at a very low rate. For alloys with a lower Mo/Cr content (e.g., 625) the possibility of pitting/crevice corrosion exists. For reasons discussed later, I do not expect MIC to be a significant process in the corrosion of the inner CRM. Although the potential for stress corrosion cracking (SCC) may be present throughout the periods of corrosion of both the CAM and CRM, it is difficult to specify if or when this process will initiate and what its effect will be on either material's time to failure.

### **CORROSION OF CARBON STEEL OUTER BARRIER**

During the hot and dry period following emplacement of the waste packages, corrosion will be extremely slow and caused by processes of dry oxidation. The development of an oxide film will serve as a "protective layer" that, if it spalls, will be reformed. With cooling of the repository (but still above the boiling point), any water that might drip on a package (for instance from a localized flow path that is able to overcome the boiling/condensation front in the rock) will react with the iron oxide, hydrolyze it, and reprecipitate iron oxy-hydroxides (e.g., FeOOH), which is a less protective oxide. With time and additional cooling, the development of persistent drips could lead to removal of the oxide and onset of enhanced corrosion. Any water that contacts the container at this time is likely to evaporate quickly and to leave behind salt deposits, but the residence time of the water on the surface is an important consideration if such drips are deemed possible. Higher corrosion rates are expected from increased residence time from frequent drips.

The temperature at which corrosion of the CAM begins is essentially the boiling-point temperature of the water contacting the surface. Because salts are likely to be in solution (from the dripping water or dissolved from salt deposits from evaporated drips on the container), the boiling point may be somewhat elevated from that of pure water.  $\text{Ca}^{+2}$  is probably the most likely cation given the concrete lining, although others include  $\text{Na}^+$ ,  $\text{Cl}^-$ , and  $\text{Si}^{+4}$ . I estimate that the temperature threshold at which corrosion of the CAM begins is

about  $110^{\circ} \pm 10^{\circ}\text{C}$ . The onset of corrosion will be distributed over this temperature range, with a higher probability of initiation at the lower temperatures.

The relative humidity at which humid-air corrosion initiates is in the range of 65 to 75 percent, as was used in TSPA-95. A normal distribution between 65 and 75 percent appears reasonable.

The relative humidity at which aqueous corrosion initiates depends on the nature of the water contact (drips versus water film) and the location on the container. I think that aqueous corrosion rates and processes are appropriate if the metal is immersed in water. This would be the case where the container is subjected to drips, especially persistent and frequent drips. For those containers judged to be subject to drips (this assessment must be made by others), I estimate that the top surface of the container—the upper 120 degrees of a cross-sectional slice—would be subject to aqueous corrosion since drips would not flow off this region of the container in response to gravity. These areas I would interpret to be subject to aqueous corrosion. The sides and bottom of the container would be subject to humid-air corrosion, not aqueous corrosion, during times of high humidity (RH higher than 85 to 95 percent). It is reasonable to assume that aqueous corrosion could not be sustained, even at high RH, on the sides and bottom of the container; however, it is conservative to assume that it would. By accepting such an assumption the possibility that water could collect at contact points between the waste package and the invert once the pedestals have collapsed is included. In a performance assessment (PA), this will mean that failure could occur at any site on a package. However, failure at a site within the upper 120 degrees of a cross-sectional slice is more probable. The site of failure in the CAM will also influence the corrosion process in the CRM. The localized acidic and saline conditions required for corrosion of the CRM will be difficult to maintain in the bottom 120 degrees of a cross-sectional slice because of the influence of gravity. Consequently, although the site of failure of either the CAM or CRM may not be important in determining the time of package failure, it is very probable (>99%) that it will be at the top. This may have a major influence on subsequent radionuclide escape times.

---

The drip frequency is very important in that it determines the difference between the rate of corrosion elsewhere on the package and the rate at the location of the drips. It will also be the major determinant of nutrient supply to sustain microbially influenced corrosion (as suggested by Little). Persistent and frequent drips can lead to spalling of the oxide and other corrosion products and the development of a preferential site for future corrosion. The corrosion rate within the area subject to drips can be ten times the rate of general aqueous corrosion. Potential formation of a mineralized "hard" crust formed from water drips may reduce or stop spalling by dripping.

The occurrence of neutral or alkaline pH conditions - and hence the mode of propagation of the corrosion front in the CAM - will vary with location on the waste package and time. Under humid air conditions, the pH will remain neutral and only uniform corrosion of the CAM will occur. For these conditions, one would expect corrosion to be uniformly distributed over the total surface of the waste package. Eventually, once dripping commences, the top surface of the container could sustain aqueous corrosion (as discussed above).

The chemistry of the water dripping on the container will be modified by permeation through concrete. The most significant influence of this process is an increase in pH (to  $\geq 10$ ) which would lead to passivation of the carbon steel (CAM) and, hence, the possibility of high aspect ratio pitting. If dripping is intermittent, water evaporation could leave salt deposits on the surface of the waste package. The wetting/drying cycles would then lead to the establishment of sufficiently saline aqueous conditions that pitting would proceed.

However, pitting is unlikely to proceed with an aspect ratio much greater than 2 (4 would be a reasonable maximum) under these wetting/drying conditions. The possibility of a pit growing, stifling and then continuing to grow at the same site through many wet/dry cycles is remote. If the availability of water is limited, the transport of dissolved corrosion products out of the pit will be minimal and their precipitation will, therefore, block the pit and stifle its growth. While growth may be restarted over a few wet/dry cycles, eventually rewetting will

be more likely to lead to the accumulation of bulk water at the edge of the pit and the uncorroded metal surface rather than at the base of the pit. Consequently, as wetting/drying proceeds, new pits will grow leading to the stringing together of a bunch of pits, rather than the continued growth of a pit of ever-increasing depth. Such a process would not allow the development of pits with a very high aspect ratio.

With time the concrete will degrade and its ability to modify the pH of permeating water will be lost. Thus, there is a finite period of time for which high pH conditions, and hence "high aspect" ratio pitting can be sustained. The duration of this alkaline period will be determined by the "alkaline capacity" of the concrete and the volume and rate of permeation of water. If the total volume of water which must permeate through the concrete in order to exhaust this "alkaline capacity" is known from laboratory experiments and the rate and volume of water permeating through the drip site in the repository is known from repository tests then the duration of the high pH, and hence pitting period, could be calculated.

Eventually, neutral conditions will be re-established. Under these conditions if pitting occurred it would proceed by the growth of hemispherical pits, and the pits grown under the previously prevailing alkaline conditions would widen as passivity was lost. Eventually these "pits" will coalesce and form a rough front that then proceeds through uniform or general corrosion. The specification of a surface roughness as outlined by Andresen and calculated by McCright is a good way to specify the movement of the general corrosion front in the CAM as a function of time. According to McCright the degree of surface roughness will decrease with the extent of corrosion of the CAM. By the time the 10-cm wall thickness of the CAM is penetrated it is very likely that the roughness factor will be small, i.e., close to one.

Given the "pit" morphologies discussed above for carbon steel, I estimate the pit density in the following way. In the case of neutral pH, I expect uniform corrosion to occur and, because there are no "pits" per se, only an advancing rough surface, there is no need to express the pit density. In the case of high pH, I estimate the average number of pits to be about 1 pit/cm<sup>2</sup> and the range from 0.1 to 10 pits/cm<sup>2</sup>. I assume a log-normal distribution to

express this range. This distribution has a mean of 1 pit/cm<sup>2</sup>; fifth percentile of 0.1 pit/cm<sup>2</sup>; and ninety-fifth percentile of 10 pits/cm<sup>2</sup>. This pit density will persist throughout the lifetime of the CAM.

## CORROSION RATES OF CARBON STEEL

I am not inclined to use a "pitting factor" to describe the rate of pitting corrosion of carbon steel. This is because there is no great difference between the depths of pits and the general corrosion front. Instead, it is reasonable to consider the pit morphology and pit density (as discussed previously) coupled with a pit growth law having the form

$$p = k t^n$$

As discussed by Scully in WPDEE Workshop 2, this type of growth law has been shown to apply to many systems, including Cr-10Ni-Ti, 304SS, Ni, CS, and Al. The value of  $n$  in the growth law expresses the range from no pits to high-aspect-ratio pits. When  $n = 0$ , general corrosion will occur; when  $n = 1$ , linear pit growth will occur. Observations of pit penetrations as a function of time show that values of  $n$  usually fall within the range of 0.33 to 0.67. A uniform distribution within this range is appropriate.

In the case of carbon steel, the total penetration depth of corrosion ( $p_t$ ) can be viewed as the combination of the penetration depth of uniform or general corrosion ( $p_g$ ) and the penetration depth of pitting corrosion ( $p_p$ ):

$$P_t = P_g + P_p$$

Under neutral pH conditions, the pitting rate is essentially zero; general corrosion is the only form that occurs. The general corrosion rate and the manner in which it is treated should follow TSPA-95.

To describe the corrosion rate at locations on the containers that experience high pH conditions, I suggest that the total penetration depth is the sum of the general corrosion depth and the pitting depth. The general corrosion rate under high pH conditions will be lower than at neutral pH. This is clear from the published literature on iron (Marsh and Taylor, 1988). The ratio by which the rate is decreased can be calculated from the values for corrosion rate in Figure 2 of Marsh and Taylor for the expected alkaline pH and the value at a neutral pH of 7. The data for general aqueous corrosion used in TSPA-95 can be multiplied (point by point) by this ratio, and a new fit determined and used. The pitting rate can be calculated from the expression given above ( $p = k t^n$ ). The values of  $k$  and  $n$  should be taken from the fit determined by Marsh et al. (1991) for penetration depths measured on naturally exposed specimens or from the NBS<sup>1</sup> database for irons and carbon steels (Romanoff, 1957).

Depths determined in electrochemically accelerated tests should not be used, because they will grossly overpredict expected behavior. To express the uncertainty in the  $n$ -value, assume that 0.48 is the mean value of a normal distribution having a fifth to ninety-fifth percentile range of 0.33 to 0.67; the distribution would be truncated at the extreme range of  $n = 0$  and 1. As pH conditions gradually become more neutral, the pitting rate will decline to the point where it becomes zero, and the general corrosion rate will increase to become that associated with neutral pH conditions. For a site subjected to a period of general corrosion and pitting under alkaline conditions and general corrosion under neutral conditions, the total wall penetration depth with time would be the sum of penetrations by all processes. The value of  $k$  could be made dependent on temperature using an Arrhenius expression of the form suggested by Scully:

$$k = k_0 \exp(Q/RT)$$

and similar expressions could be used to express the dependence on other factors likely to influence pitting, such as the chloride to sulphate concentration ratio in the groundwater. Unfortunately, these relationships are not known. Even in the case of temperature, when a

---

<sup>1</sup> National Bureau of Standards is now known as the National Institute of Science and Technology (NIST).

---

simple Arrhenius relationship of this form would be anticipated, there is no clear evidence that such a relationship applies. Thus, Marsh et al. (1991) found that the depths of pit penetration in carbon steel were lower at 90°C than at 25°C. A possible explanation for such an inverted temperature-dependence is that the processes retarding pit growth are accelerated more by temperature than those which accelerate it.

However, it is noteworthy that the expected temperature-time profile for the container surface shows that the temperature will not change much over the period when the CAM is expected to be subject to pitting. There seems little point, therefore, in attempting to include a temperature-dependence for pitting.

#### **ALTERNATIVE CORROSION-ALLOWANCE MATERIAL**

The database available to describe the general corrosion behavior for Monel 400 is very sparse compared to that for carbon steel (TSPA-95). Clearly, an advantage could be gained by using Monel 400 rather than carbon steel. The corrosion behavior of Monel 400 has been reviewed in detail by McCright (WPDEE Workshop 3). I do not recommend the use of Monel 400 for the following reasons.

- (1) It is at least one order of magnitude more expensive.
- (2) The available data for carbon steel allows the use of a justifiable rate of corrosion as a function of time to be used in PA calculations. Such a fitted expression could not, at present, be derived for Monel 400.
- (3) Such a substitution would remove the best and most extensive database from PA calculations and weaken the credibility of a process already fraught with limitations due to lack of data.

#### **CORROSION OF CORROSION-RESISTANT INNER BARRIER**

The potential for initiation of corrosion of the corrosion-resistant material (CRM) begins with the first penetration of the corrosion-allowance outer barrier. A realistic model would be to

assume that corrosion sites on the CRM initiate according to the evolution of corrosion penetrations through the CAM outer barrier. Therefore, corrosion sites would initiate where CAM pits penetrate the 10-cm thickness of the CAM, as defined by the following:

$$t_{\text{init}} = t_{\text{F}} + t_{\text{GP}}$$

where  $t_{\text{init}}$  is the time it takes to initiate corrosion at a site on the CRM;  $t_{\text{F}}$  is the time for the CAM to fail at that site; and  $t_{\text{GP}}$  is the period of galvanic protection, if any. Following the period of galvanic protection, general and/or localized corrosion of the CRM will occur depending on the chosen material and the conditions established at the failure site in the CAM.

Whether galvanic protection will occur is uncertain. My conclusion is that the period of galvanic protection will be limited, primarily due to the morphology of "pits" and the general corrosion front in the carbon steel. In some cases where the aspect ratio of a pit is relatively high, the initial conditions for galvanic protection may be favorable. On first penetration of the CAM, especially at the site of a deep pit, only a small area of the CRM would be exposed. If it is assumed that a bulk aqueous solution having a high chloride concentration exists within the pit, a dubious prospect at best, then a galvanic couple could be established between the CRM and the CAM. The area of the anode (CAM), which comprises the pit walls, would be large. The area of the cathode (CRM) would be small. This combination would be ideal for galvanic protection. However, as the couple functioned the CAM would be consumed by corrosion and the area of exposed CRM would increase. Under these conditions the function of the galvanic couple would be impaired; i.e., the anode-to-cathode ratio would decrease.

As discussed previously, the expected aspect ratios of "pits" in the CAM carbon steel are low; except for the case in which the canister surface has high-pH drips, the morphology of corrosion is one of a rough surface, not high-aspect-ratio pits. Thus, after the CAM is penetrated, a relatively short period is expected before the "pit" widens and exceeds the throwing distances expected between the CAM and CRM. This throwing distance, i.e., the

range of protection for the CRM, is expected to be a few millimeters at best. I estimate that the period of galvanic protection for general corrosion of carbon steel (i.e., no high-aspect-ratio pits) would be about 50 to 150 years. Even in the case where high-pH drips lead to localized pitting, the expected aspect ratios are 2 to 4. I expect there to be little time before the pit widens and the protection is lost. In such cases I expect that the period of galvanic protection would last no more than 300 years.

Given a penetration of the CAM, a number of factors determine the probability that localized corrosion of the CRM will initiate. These factors include the availability of water,  $\text{Cl}^-$  content, pH,  $\text{Fe}^{3+}$ , temperature, and  $\text{O}_2$  and the susceptibility of the material chosen. The probability of initiation is essentially the probability that an aggressive environment will exist relative to these factors. Water availability will depend on whether the canister experiences drips and whether we consider the top, sides, or bottom of the canister. The  $\text{Cl}^-$  content may be high, at least initially, at those sites that experienced dripping on the CAM, evaporation, and development of a salt scale. Ferric ions,  $\text{Fe}^{3+}$ , will be present due to dissolution of the carbon steel corrosion products. These corrosion products will be a mixture of  $\text{Fe}^{2+}/\text{Fe}^{3+}$  oxides, e.g.,  $\text{Fe}_3\text{O}_4/\text{Fe}_2\text{O}_3/\text{FeOOH}$ . If bulk water exists in the CAM failure site, then the solubility of these oxides will yield a solution saturated by a mixture of  $\text{Fe}^{2+}$ ,  $\text{Fe}^{3+}$ , and hydrolyzed species of these two ions (e.g.,  $\text{FeOH}^+$ ,  $\text{FeOH}^{2+}$ ). This will buffer the redox potential at the surface of the CRM. This buffering will protect the CRM from localized corrosion for a short period. At a guess, this period will be short because the continuing availability of  $\text{O}_2$  will lead to the total oxidation of these oxides, and the redox buffering capacity will disappear.  $\text{O}_2$  access to the CRM surface probably is transport-limited because of the thick outer deposit of CAM corrosion products.

In the absence of an extensive usable database for the localized corrosion of the various nickel alloys considered as candidate materials, it would be judicious to choose an alloy with a high Cr/Mo content. The table given by Andresen of critical temperatures for the initiation of pitting/crevice corrosion on Alloys C22, C276 and 625 under aggressive conditions clearly indicates the advantages of the use of an alloy high in Cr and/or Mo. If either C276 or C22 is chosen it is very unlikely that localized corrosion would initiate. Consequently, degradation

of these alloys would be by general passive corrosion and would be expected to proceed at very low rates. The rates given by McCright for the general passive corrosion of 825 (a more corrodible alloy) suggest this general corrosion rate could be as low as 0.1  $\mu\text{m}/\text{year}$  or less. As stated by McCright, one would expect the Ni-Cr-Mo alloys to have lower rates making the adoption of the values for 825 conservative. It would be judicious to assume these rates would not decrease with time. The passive corrosion rate should be uniformly distributed about a value of 0.1  $\mu\text{m}/\text{year}$  with an associated  $\sigma$  value of  $\pm 0.9$ .

While this scenario seems quite reasonable it may be considered unrealistically optimistic by some based on the sparse database of rates and the incomplete understanding of passive corrosion behavior. In view of these uncertainties it would be judicious to consider that localized corrosion of these materials is possible at failure sites in the CAM.

Corrosion tests show that alloy I-625 does not experience pitting in aggressive environments unless the temperature is higher than 80°C. For alloy C-22, the threshold temperature is 100°C. However, I consider crevice corrosion to be a more probable process than pitting, and this process can initiate at lower temperatures than pitting. I suggest that crevice corrosion be assumed to initiate if T is  $>75^\circ\text{C}$  for alloys such as C22 and C276 when the CAM fails and the short galvanic protection period is over. The probability of initiation should be set at one at 75°C and decrease exponentially to zero at 65°C. This probability can be considered a site-to-site probability; i.e., if  $T \geq 75^\circ\text{C}$ , every site exposed by failure of the CAM will initiate a crevice. Once initiated, it will grow with the growth law discussed below. If  $T \leq 65^\circ\text{C}$ , no exposed site will initiate a crevice, and the CRM can be assumed immune to localized corrosion, and will corrode passively at the rate specified in the previous paragraph.

In subsequently determining the time to failure of the CRM, only the first crevice initiated matters, since this is assumed to continue to penetrate the CRM for the longest period. This scenario includes, therefore, the implicit, very conservative assumption that no crevice will stop growing. This is clearly a conservative assumption for high Mo Ni-alloys for which the

---

propagation of localized corrosion processes is generally limited by changes in alloy composition at localized corrosion sites (pits/crevices). It may be possible to demonstrate that localized corrosion will be stifled based on a relatively rapid experimental program.

Although only the first crevice to initiate matters, one could include a distribution of propagating crevices. This distribution would be defined by the distribution of penetration sites in the CAM. For the reasons discussed above, I would consider only crevices on the top of the waste package. Assuming that pit/crevice corrosion initiates, the pits/crevices propagate according to growth laws similar in form as those for the CAM. Experience with corrosion-resistant alloys shows that initial penetration rates usually are relatively high and, because the conditions conducive to penetration are not sustained, the rate decreases with time. For example, the penetration rates for titanium Ti-2 start at about 600  $\mu\text{m}/\text{yr}$  and decrease to values  $<10 \mu\text{m}/\text{yr}$  quite rapidly (plot of maximum pit depth versus time presented by D. Shoesmith at WPDEE Workshop 1); see also Shoesmith et al. (1995).

In the absence of similar growth laws developed for the corrosion-resistant materials of interest (e.g., C-22), I suggest that this growth law for Ti-2 be used to provide a conservative estimate of the possible penetration rate of the CRM by crevice corrosion. This damage function was developed using a galvanic coupling technique in deaerated saline solutions at 100°C (Shoesmith et al., 1995).

The conditions in these tests can be considered aggressive compared to those anticipated in the repository. This is especially true for the supply of oxygen which is unimpeded in the free solutions used experimentally, but would be expected to be accessible to corrosion sites on the CRM by slow transport through the accumulated corrosion products of the CAM. The use of this "damage function" for Mo-containing Ni-alloys is very conservative since Grade-2 Ti possesses no metallurgical features capable of suppressing the penetration rate. Of the candidate materials for the CRM, 625 could exhibit similar behavior but C276, C4, C22 would not be expected to penetrate at such rapid rates. The form of this crevice growth rate (damage function) could be expressed in a similar form to that used for pitting (i.e.,  $P = kt^n$ ) but is better represented by a function of the form

$$P = k \log t - x_0$$

where P is in microns, t in hours and  $x_0$  is the uncertainty in the origin for this fit to the data. For the limited available data  $k = 750 \pm 290$  and  $x_0 = -1200 \pm 800$ .

Although stress corrosion cracking (SCC) cannot be ignored, it is difficult to see how it should be included in the modeling of waste package degradation. One way to include its possible effect is to consider that cracks may develop at the base of a well-developed pit/crevice and accelerate the pitting/crevicing process.

It is less likely that crevice corrosion will be stifled than that pitting corrosion will be. The local chemistry required to sustain pitting is more easily lost in a pit than in a crevice. The controls on the probability of stifling are the following: limited oxygen transport through the CAM corrosion products; limited water; gradually decreasing temperatures; and the metallurgical properties of the CRM. Of these, arguments based on temperature and/or metallurgical properties are easiest to test experimentally or to make by rational argument, since they are independent of the uncertainties in repository conditions.

Because of the relatively high pit/crevice spatial density assumed for the CRM (~10 pits/cm<sup>2</sup>), the advancing corrosion front will almost resemble a general corrosion front. This means that after sufficient penetration of the inner barrier, failure of the waste package may occur by collapse of the container wall. Scenarios for wall thickness collapse have been developed for the Canadian waste package. However, the Canadian container is subject to large external pressures due to its location below the water table in a compacted clay. This will not be the case at Yucca Mountain. However, given the evidence that localized corrosion can be followed by SCC, I suggest the following assumption. Only two-thirds of the wall thickness of the CRM should be considered available for crevice corrosion (i.e., 13 mm). Once penetration by crevice corrosion exceeds this, the package is assumed to fail rapidly by SCC.

---

## **MICROBIOLOGICALLY INFLUENCED CORROSION**

According to Little, microbiologically influenced corrosion (MIC) affects the probability of initiation but not the rate of corrosion. Tests have shown that it is inevitably possible in the laboratory to feed microbes the proper nutrients to flourish. The key issue, then, is to characterize the environment of the potential repository as a function of time and to ascertain whether proper conditions for MIC will prevail. Studies by Sim Gascoyne have shown that the amount of available water is a limiting factor, as is the supply of nutrients. As shown schematically on Figure DS-2, MIC will not occur in the early history of the repository because of elevated temperatures and low relative humidity. After temperatures decline and humidity increases, the amount of MIC will be limited in a humid air environment having no drips on the waste package. This is because beneath the porous oxide covering the CAM, free water is limited, and it will be difficult to get nutrients to the fresh surface beneath the oxide, thus limiting the potential for developing a biofilm. However, under a dripping water scenario there will be more rapid access to the interface and a larger potential for MIC. I am not sure of the effect microbes would have on the oxide.

After the 10 cm of the CAM have been corroded, I believe that it will be very difficult for water and nutrients to reach the interface with the CRM. Therefore, I dismiss MIC as a consideration for the CRM, except in the case of water dripping on the waste package.

The choice of a material such as C-4 or C-22 for the CRM reinforces this argument, as MIC is not found on these materials. Also, since they are assumed to corrode locally by crevice corrosion, the initiation process that might be influenced by MIC is already taken to be instantaneous, and MIC is not expected to accelerate the propagation (penetration process). Consequently, the conservative localized corrosion scenario described above for the CRM will not be influenced by MIC.

I do not think that MIC will influence rates of pit penetration for the CAM for the same reason I do not think it will affect crevice propagation in the CRM. In the short term, I think

MIC could accelerate the general aqueous corrosion of the carbon steel. Based on nutrient-fed experiments (i.e., very conservative conditions), a maximum enhancement factor of 4 to 5 has been measured. This factor could be applied initially and assumed to decrease exponentially with time. I would assume MIC to be negligible after 500 years.

## **OTHER ISSUES**

### **Radiolysis**

The most effective way to consider possible effects of radiolysis is to look at the dose rate (assuming a half-life of 30 years of Cs-137, which is the dominant radionuclide contributing to radiation dose) at the time that package surface temperatures have declined to about 110°C and relative humidity is about 65 percent. Based on such considerations, if the container remains dry for 1000 years the dose rate at the package surface will have decreased from an initial value of 50 to 100 Rad/h to a totally insignificant level. Consequently, by the time the humidity reaches a level that radiolysis of moist air could produce acidic oxidizing conditions, the radiation dose rates will be too low to be significant.

### **Welds**

I do not expect enhanced corrosion in a weld in the CAM if it is done properly. For the CRM, the weld could be a more susceptible corrosion site. However, I think the scenario for localized corrosion outlined is already sufficiently conservative to cover any enhanced weld susceptibility.

### **Ceramic Coating**

I do not recommend the use of a ceramic coating. Its failure at one site would destroy its effectiveness, since penetration at that one site would have to be assumed to advance at a rate determined from the scenario outlined above. I do not think that it will be possible to claim absolute containment for a significant period of time on the basis of available information.

## REFERENCES

- Marsh, G.P., and Taylor, K.J., 1988, An assessment of carbon steel containers for radioactive waste disposal: *Corrosion Science* 28(3), p. 289-320.
- Marsh, G.P., Taylor, K.J., and Harker, A.H., 1991, The kinetics of pitting corrosion of carbon steel applied to evaluating containers for nuclear waste disposal: SKB Technical Report, 91-62.
- Romanoff, M., 1957, *Underground Corrosion*: NBS Circular 579.
- Shoesmith, D.W., Ikeda, B.M., Quinn, M.J., and Kolar, M., 1995, Estimating the lifetimes of titanium containers for nuclear fuel waste: A damage function for the crevice corrosion of Grade-2 titanium: Atomic Energy of Canada Limited Report, AECL-11255, COG-95-18.

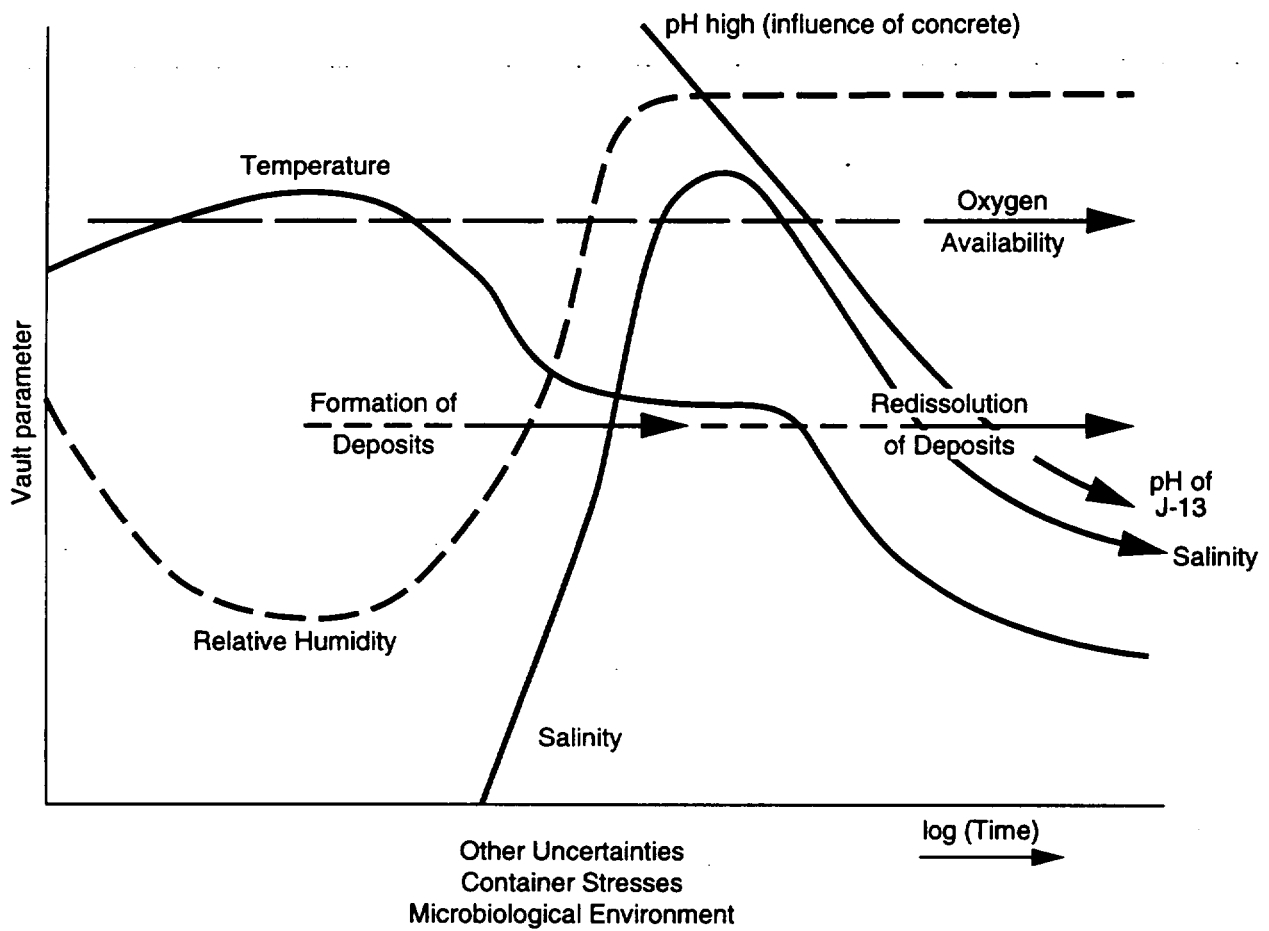


Figure DS-1 Schematic diagram of changes in key conditions with time

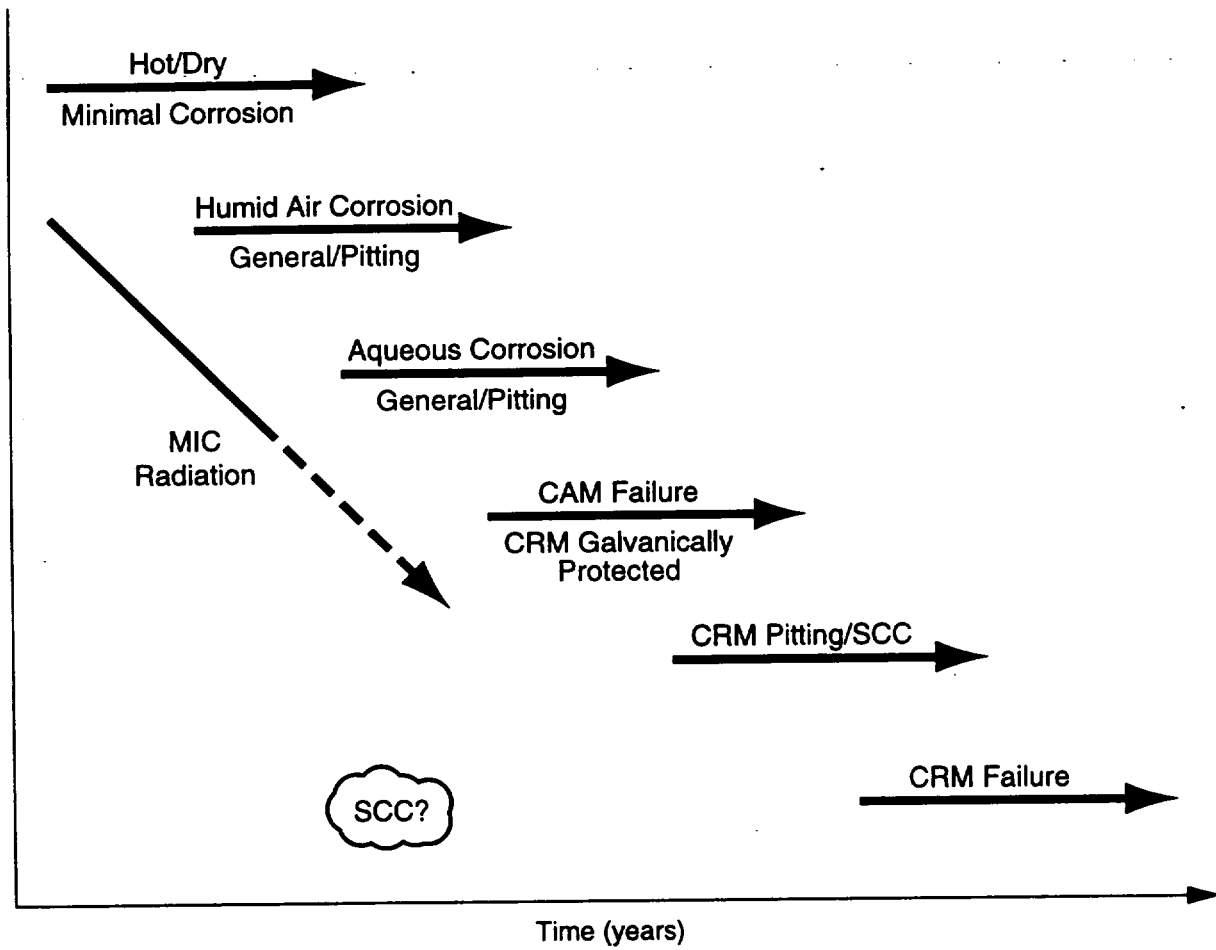


Figure DS-2 Schematic diagram of evolution of corrosion processes

**APPENDIX E**  
**QUALITY ASSURANCE**

## QUALITY ASSURANCE

The Waste Package Degradation Expert Elicitation Project was completed under the Quality Assurance Program for the Civilian Radioactive Waste Management and Operating Contractor (CRWMS M&O). The process and procedures for M&O staff conducting the activity were defined in the Project Plan for this expert elicitation project. Section 2.0 of this report summarizes the process for eliciting expert judgments. As discussed in Section 2.0, formal guidance for the process of expert elicitation has been established and this guidance has been successfully applied in other comparable assessments.

## **QUALITY ASSURANCE**

The Waste Package Degradation Expert Elicitation Project was completed under the Quality Assurance Program for the Civilian Radioactive Waste Management and Operating Contractor (CRWMS M&O). The process and procedures for M&O staff conducting the activity were defined in the Project Plan for this expert elicitation project. Section 2.0 of this report summarizes the process for eliciting expert judgments. As discussed in Section 2.0, formal guidance for the process of expert elicitation has been established and this guidance has been successfully applied in other comparable assessments.